Techno-economic and exergetic assessment of an oxy-fuel power plant fueled by syngas produced by chemical looping CO_2 and H_2O dissociation

Azharuddin Farooqui[ac], Archishman Bosea[b], Domenico Ferrero[a], Jordi Llorca[c], Massimo Santarelli[ab]

[a]Energy Department (DENERG), Politecnico di Torino, Corso Duca degli Abruzzi 24, Torino, 10129, Italy

[b]Department of Energy Technology, KTH Royal Institute of Technology, Brinellvägen 68, 10044 Stockholm, Sweden

[c]Institute of Energy Technologies, Department of Chemical Engineering and Barcelona Research Center in Multiscale Science and Engineering, Universitat Politècnica de Catalunya, EEBE, Eduard Maristany 10-14, Barcelona 08019, Spain

Abstract:

Natural Gas Combined Cycle (NGCC) are presently the most efficient fossil power generation units. The efficiency penalty resulting from integration of carbon capture and storage (CCS), is however, a major challenge. The present study a oxyfuel NGCC integrated with Chemical looping syngas production (OXY-CC-CL), for power generation with CCS. In this system, the chemical looping CO_2/H_2O dissociation (CL) for production of syngas (CO and H_2 with methane reduction step in redox cycle) from recycled exhaust gas within the power plant. The aim of the present work is to assess the thermodynamic (both energetic and exergetic), economic and environmental performance of the integrated chemical looping unit oxyfuel NGCC power plant with carbon capture. A 500MW scale plant was modelled and compare with a conventional NGCC and oxyfuel NGCC plant with carbon capture (OXY-CC). The net efficiency penalty of the proposed OXY-CC-CL unit was 4.2% compared to an efficiency penalty of 11.8% of the OXY-CC unit with a 100% carbon capture. The energetic efficiency obtained hence was 50.7%, together with an exergetic efficiency of 47.1%. However, system optimization with heat integration via revealed the possibility to increase the system efficiency by up to 56%. Sensitivity analyses were performed with regards to system operational parameters to identify relative impacts. The specific capital cost of the proposed OXY-CC-CL was obtained as 2455 $/kW, with a corresponding LCOE of 128 $/MWh without carbon tax. The cost of CO_2 capture was obtained at 96.25$/tonne$CO_2$,

comparable to state of the art CCS processes. The environmental impacts of the system were also evaluated, with the water and land footprints being higher than conventional NGCC.

Keywords: Oxyfuel combined cycle, Chemical looping syngas production, Thermodynamic Analysis**,** Techno-economics, Carbon Capture and Storage

1 Introduction

Burning fossil fuels, resulting in anthropogenic carbon dioxide (CO_2) emissions are presently recognised as the primary contributor to climate change, with 36.2 Gt being emitted in 2016 [1–3]. Notwithstanding substantial investment and decline in prices of renewable energy, fossil fuels continue to play an indispensable role in the World's energy landscape [4]. Indeed, even though the trend is on a decline, such technologies continue to play a major role as the primary energy source, especially in developing countries [5]. Hence, it is expected that the relevance of fossil fuels in the primary energy mix will continue to a significant extent in the considerable future.

Carbon capture and storage (CCS) technologies have been shown to have considerable potential to reduce such anthropogenic CO_2 emissions as part of the global transition towards a low carbon energy system [2,6,7]. These technologies are typically categorized into three categories: pre-combustion, post-combustion, and oxy-combustion [8,9], the common idea being the CO_2 capture and subsequent storage from the complete or partial combustion of fossil fuels from either the power or industrial sectors. The captured CO_2, nevertheless, needs to be subsequently compressed to approximately 110 bar prior to transportation via pipeline to a storage site [2,10,11]. However, in recent studies, recycle and re-use of the captured CO_2 via innovative methods such as chemical formation for subsequent use [12–14], has also received much attention as an alternative to storage. .

The oxy-fuel combustion is currently one of the most promising alternatives among the portfolio of all the low-emission technologies (LETs) [15,16]. In this technology, the fuel (coal or natural gas or bio-methane) is burnt in an oxygen (O_2) rich environment (near stoichiometric O_2 flows), instead of air, thereby improving combustion efficiency [17] and eliminating NOx emissions and generating only CO_2 and H_2O as the product of combustion

unit. The oxygen is supplied via an air separation unit (ASU). Burning fuels under these conditions generate combustion gases, which after condensation yields a very high purity of CO_2 exhaust. Oxy-combustion can also be applied to natural gas combined cycle (NGCC), however, subject to the redesign of gas turbines, because alternation in the physical properties of the metal occurs due to the increased CO_2 concentrations in the flue gas [11,17]. Nevertheless, ease and ability to retrofit existing systems at low cost are the primary attractions towards such systems [16], together with the high efficiency of 96-99% carbon capture [18].

Similar to LETs, technical challenges exist for the oxy-fuel combustion process. The most critical limitations lie in the higher energy penalties associated with air separation unit (ASU) for O_2 production and CO_2 processing unit (CPU) for CO_2 purification and compression [2,19,20] after the combustor unit. The existing commercialized technology for air separation for utility-scale application is the cryogenic air separation process (CASU). It works on the principle of the cryogenic distillation via compression of air to its liquefaction stage, followed by the fractional distillation of its constituent components, such as N_2, O_2, Ar and other rare gases. The primary advantage is that this process can produce liquid or gaseous streams of N_2 and O_2 as per the specification of the end user and for large-scale requirements also. Indeed, O_2 production, via such a process of cryogenic distillation of air, demanding 160 to 250 kWh per ton of O_2 produced [21,22] is acknowledged as the bottleneck [2,16]. The efficiency loss after integrating the ASU unit to make the oxy-fuel combustion power unit would be 13% compared to the conventional NGCC unit without carbon capture [23]. The penalties incurred by the use of ASU could easily offset any advantages gained by oxyfuel combustion prompting many researchers to investigate the use of alternative air separation systems. However, to date, none of the alternative technologies for air separation have been able to produce high purity oxygen at large utility scale, either due to high costs, such as for adsorption processes, or the technology is still under development or in demonstration stage, as for membrane technologies such as oxygen transport membranes [24,25]. State of the art of ASU can consume between 10 and 40% of the gross power output after retrofitting a conventional coal-fired power, resulting in a net energy penalty as high as 8-13 percentage points [7,26]. True, with a lower purity of O_2 of about 95%, if acceptable for such oxy-fuel applications, the energy requirement for oxygen production with ASU can be further reduced, together with the energy penalty [16].

Several studies of different schemes have been proposed to increase the efficiency for carbon capture. Improving the efficiency through a novel chemical looping air separation technology has been proposed by Moghtaderi [22]. From a system perspective, chemical looping combustion has been shown to have considerable potential for a relatively high efficiency of power production together with carbon capture. For a pulverized coal power plant, around 39% efficiency was calculated while ensuring a CO_2 capture efficiency of almost a 100% [27]. Innovative system integration has shown further possibility to decrease the energy penalty of carbon capture.

Natural gas combined cycle (NGCC) power plants are among the most efficient fossil fuel-fired power plants, able to reach net efficiencies of up to 57% based on the Lower Heating Value (LHV) of the fuel [28]. Correspondingly, the specific CO_2 emissions are low as well compared to other fossil fuel power generation units, at around 350 gCO_2/kWh, besides having much less SO_x and NO_x emissions due to the lower Sulphur and Nitrogen content of the fuel [28]. Addition of CCS units to considerably decrease the specific CO_2 emissions to much below 100 gCO_2/kWh have therefore been studied and presented in multiple literatures via diverse technologies [28–30]. Like solid fuel power units, the primary motivation of such studies included the decrease in the energy penalty of the capture process, thereby increasing the efficiency of the power plant alongside keeping the capture efficiency to its maximum potential.

Chemical looping for thermo-chemical dissociation of the captured CO_2 has received considerable interest in the last couple of years after the initial success of the thermochemical water splitting [31]. In fact, the simultaneous splitting of CO_2 and H_2O, resulting in the formation of a syngas has great potential to improve the system efficiency by providing additional fuel with high calorific value leading to CO_2 recycling. Chemical looping CO_2/H_2O splitting, like chemical looping combustion (CLC) cycles, use metallic oxygen carriers to convert the thermo-chemical energy into chemical energy [32]. The cycle can either be driven by concentrated solar energy or through the chemical energy of methane, the latter having multiple benefits, besides a low-temperature reduction of metal oxide than direct thermal reduction [33,34]. A basic schematic of the methane driven Chemical Looping CO_2/H_2O splitting is shown in Figure 1.

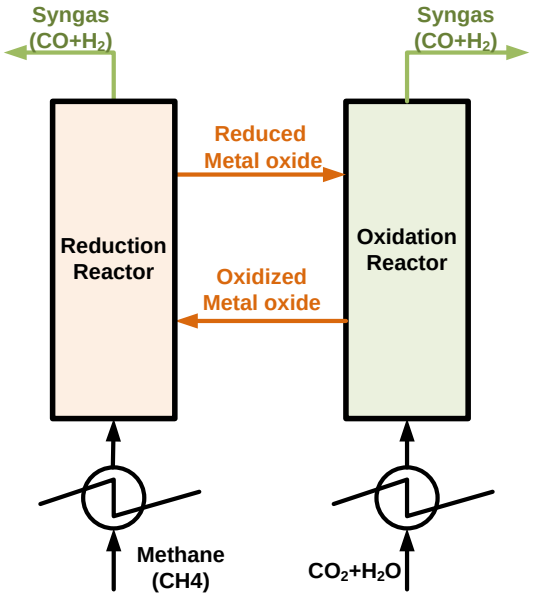

Figure 1 Conceptual scheme of the chemical looping syngas production through methane reduction and corresponding splitting of water and carbon dioxide, usually present in waste gas from industrial applications

In the reduction step (eq. 1), the metal oxide is reduced in the presence of methane, either up to stoichiometric or a non-stoichiometric extent, δ. The δ moles of oxygen released from the MeO_x forms CO and H_2 by partial oxidation of CH_4. In the subsequent reaction steps, usually exothermic, (eq. 2), $MeO_{x-\delta}$ reacts with CO_2 and/or H_2O to reincorporate oxygen into the metal oxide lattice, while reducing the CO_2 and/or H_2O into a stream of syngas (CO or H_2 respectively). Reactions (2a) and (2b) can be intrinsically assumed to result in complete oxidation at thermodynamically favourable temperatures depending on the metal oxide redox pairs. The oxygen production during the first step depends on the reduction extent and the metal cation highest valence that be reduced. Highest possible dissociations are in principle sought, the higher the oxygen released during dissociation the higher oxygen taken from CO2 and H2O during oxidation.

$$\text{Methane}-\text{reduction}: MeO_x + \delta CH_4 \rightarrow MeO_{x-\delta} + \delta\left(CO + H_2\right) \quad (1)$$

$$\text{Water}-\text{splitting(WS)}: MeO_{x-\delta} + \delta H_2O \rightarrow MeO_x + \delta H_2 \quad (2a)$$

$$CO_2-\text{splitting(CDS)}: MeO_{x-\delta} + \delta CO_2 \rightarrow MeO_x + \delta CO \quad (2b)$$

In this regard, multiple studies have been reported in the literature to identify the most suitable metal oxide redox pairs [34–36] and reactor scale experimental analysis for reactor modelling [32,34]. These include volatile metal oxide/metal system such as ZnO/Zn; SnO/Sn or non-volatile metal oxide/metal oxide pairs such as Fe_3O_4/FeO; Mn_3O_4/MnO; CeO_2/Ce_2O_3, etc. Other metals oxides tested are ferrites with different valences, Co_3O_4, Nb_2O_5, WO_3, SiO_2, In_2O_3, CdO to name few [32,37–41].

Cerium (IV) oxide (CeO_2) is extensively studied for thermochemical redox application due to its strong ability to undergo cyclic redox reactions having retain its chemical and structural properties aside from resilience to mechanical stress and agglomeration, attrition resistant [42]. Rapid kinetics, together with the very minimal effect of sintering at high temperature with good attrition resistance and mechanical strength makes ceria the state of the art among the non-volatile redox pairs for H_2O splitting application, which can be further exploited for large-scale applications. The stoichiometric redox system of Ce_2O_3/CeO_2 was explored and found to have a high temperature for reduction of 1650 K. However, non-stoichiometric reduction of ceria ($CeO_2 \rightarrow CeO_{2-\delta}$) occurs at a relatively lower reduction temperature of 1673 K [40]. Ceria is reported to have favourable oxidation kinetics, but it has the drawback of poor thermal reduction ability at lower temperatures. Therefore, it is suggested to reduce with fuel such as methane undergoing partial oxidation producing syngas during both reduction and oxidation step, thereby improving the syngas production and lowering operating temperature.

Plant scale analysis of chemical looping combustion coupled with NGCC for carbon capture has been analysed with a net electrical efficiency of 43%, an energy penalty of 14%-points with respect to the NGCC plant without capture [43]. However, till date, as per the knowledge of the authors, no complete system analysis of the NGCC power system with the chemical looping (CL) CO_2/H_2O splitting unit has been studied for utility-scale applications. Furthermore, existing literature, comparative evaluation of individual capture technologies is difficult due to variations in modelling assumptions regarding the type of fuel used, the scale of power output and efficiencies of individual process units. In the present work, an Oxy-fuel combustion power plant integrated with a chemical looping CO_2/H_2O dissociation (OXY-CC-CL) unit has been proposed and evaluated. The results have been compared with a conventional NGCC without carbon capture and an Oxyfuel-combustion power plant (OXY-CC) with carbon capture technology through simulation studies via common modelling

assumptions and considerations. The two capture technologies were analysed against a conventional NGCC process without capture to estimate and compare, besides the energy penalty associated with CO2 capture, economic and other environmental impacts as well. An overall exergetic performance comparison was also performed for the NGCC, OXY-CC and OXY-CC-CL processes to compare the plant performance. A detailed exergetic study was carried out for the proposed system separately to identify the sources of irreversibility in each process, and hence, the scope for improvement and optimization. Power production, power consumption, electrical efficiency, CO_2 capture efficiency, exergy, economic performance, land and water footprint are the key parameters investigated and their variation is reported in the present work.

2 Methodology

The present study performs a techno-economic and sustainability assessment of the proposed Oxyfuel-chemical power plant with Carbon Capture integrated with chemical looping CO_2 and H_2O splitting (OXY-CC-CL) compared to state of the art NGCC and oxyfuel-CC with carbon capture. Based on the literature reported CeO_2 is selected as oxygen carrier.

In this process, to integrate the system with a traditional oxyfuel power plant, methane reduction of ceria has been considered as an alternative to thermal reduction. Ceria reduction, even though non-stoichiometric, tends to approach stoichiometric conditions at temperatures beyond 1400^{o}C when reduced with methane. Recently one experimental study reported that CeO_2 reduced to Ce_2O_3 above 900^{o}C completely when reduced with methane [44]. Though this claim is subject to investigation based on the size of the material and quantity of the material chosen and microstructural studies were missing. In the present study, a thermodynamic redox pair of CeO_2/Ce_2O_3 for stoichiometric reduction of ceria for maximum redox pair utilization was considered to evaluate the highest possible performance of the integrated system. Accordingly, the CeO_2/Ce_2O_3 redox pair with reduction of CeO_2 in the presence of methane, and subsequent oxidation with CO_2/H_2O was utilized, as described by the equations (3-4).

$$\text{Methane reduction: } 2CeO_2 + CH_4 \rightarrow Ce_2O_3 + CO + 2H_2 \quad (3)$$

$$\text{Water-splitting(WS): } Ce_2O_3 + H_2O \rightarrow 2CeO_2 + H_2 \quad (4a)$$

$$CO_2\text{-splitting (CDS): } Ce_2O_3 + CO_2 \rightarrow 2CeO_2 + CO \quad (4b)$$

In the reduction reactor, the methane reduces the metal oxide at a higher oxidation state (CeO_2) to a lower oxidation state (Ce_2O_3), while itself getting oxidized to CO and H_2 via reaction (3). The reduced ceria is then recycled back to the higher oxidation state through reactions (4a) and (4b). In both the reactors, syngas was generated, however, with varying H_2/CO fractions.

Based on the above selections, the system performance and techno-economic assessments of the OXY-CC-CL power plant were carried out as per the methodology, depicted in Figure 2. It should be stressed that several alternative plant configurations, differing in strategies for integration of the CL unit to the traditional system and subsequent mode of utilization of the syngas generated from the oxidation reactor were conceptualized and examined. However, all possible combinations of interest could not be presented within the scope of the present work. The assessments presented herein were performed using a combined Aspen Plus model and an in-house spread-sheet developed specifically for the current study.

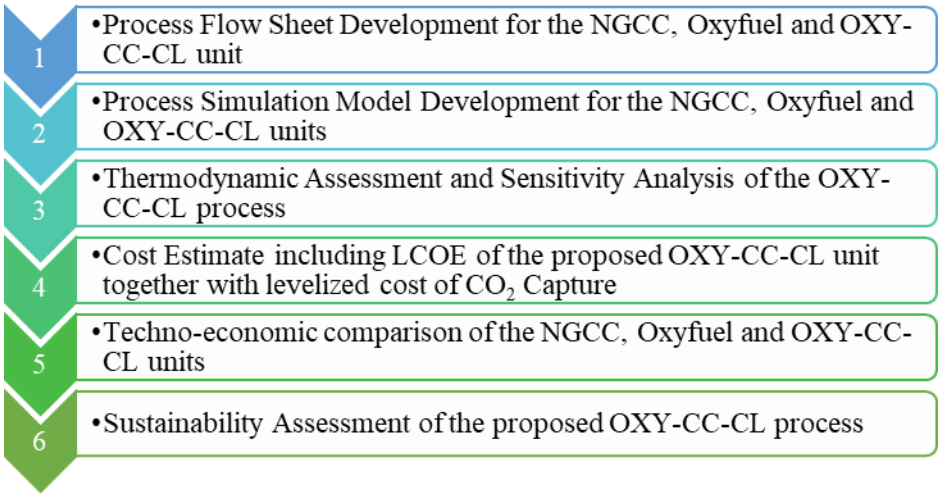

Figure 2 Methodology for Techno-economic and Sustainability Assessment

The process evaluation, techno-economic study and sustainability assessments summarized in this paper does not include considerations of retrofitting existing state of the art NGCC or oxyfuel NGCC power plants. This is due to considerable complexity identified for such integrations, which can be found within the explanations of the subsequent sections.

The process simulation models and corresponding technical analyses were developed in Aspen Plus®, version 8.4. to investigate the performance of the proposed system (OXY-CC-CL) in comparison to the traditional plant configurations (NGCC and oxyfuel combustion base NGCC (OXY-CC)). The key technical performance indicators evaluated are (i) plant

thermal efficiency, (ii) plant thermal efficiency penalty, and (iii) relative efficiency gain, (iv) plant exergetic efficiency and (v) plant-specific emission savings.

The economic assessment of the proposed OXY-CC-CL unit with the corresponding comparison with NGCC and OXY-CC with Carbon capture was performed based on the different cost data available in the literature. The key economic performance indicators being evaluated are (i) power plant capital cost, (ii) operating costs, (iii) Levelized Cost of Electricity (LCOE) and (iv) cost of CO_2 avoided as Levelized Cost of CO_2 Savings. Besides techno-economic assessment, sustainability assessment through water and land footprint assessment was performed based on existing methodologies available in the literature.

3 Process Description and Plant Configuration

Figure 3 presents the block diagrams of the conventional NGCC, OXY-CC and the novel CL coupled Oxyfuel (OXY-CC-CL) process. The process description of the traditional NGCC and OXY-CC are outside the scope of this text and can be found in multiple kinds of literature [29,43]. A complete CL integrated novel Oxyfuel NGCC power plant (OXY-CC-CL), comprising several operating units including the reduction reactor (RED) and the oxidation reactor (OXI), as integral parts of the CL unit, together with traditional units of an oxyfuel power plant including cryogenic ASU has been proposed and described in the following section.

The heart of the proposed OXY-CC-CL plant is the chemical looping CO_2/H_2O splitting unit (CL). The CL unit works at a considerably lower pressure than that of the natural gas supply of around 70 bars from the gas networks from the outside battery limit (OSBL). Therefore, the gas needs to be expanded to the working pressure of the CL unit. Pre-heating of the inlet natural gas by the process heat of the power plant can considerably improve the net work obtained by such expansion. The expanded methane is further pre-heated and supplied to the reduction reactor (RED) where it is partially oxidized into CO and H_2, producing syngas, while reducing the cerium (IV) oxide to cerium (III) oxide as per equation (3). The selection of the operating temperatures is crucial to prevent the complete oxidation of the methane to CO_2 and water, simultaneously preventing carbon deposition through methane cracking.

The reduction reaction is highly endothermic, requiring a large amount of supplemental heat to maintain the reforming temperature and drive the reaction forward. The metal oxide reduction by methane is preferably operated at elevated temperatures of above $900^{o}C$ to

ensure more than 99% conversion of the methane to CO and H_2. However, it has been observed from thermodynamic studies that around 40% to 60% excess flow of methane is necessary to ensure complete reduction of metal at temperatures below 950^{o}C. As also deduced from the same study the most suitable methane to ceria (CH_4/CeO_2) flow ratio was 0.7, higher than the stoichiometric ratio of 0.5, and was hence selected for the present system deployment. As for the pressure, multiple advantages and disadvantages exist for systems working at higher pressures. While solids handling is a major challenge for higher pressure, the previous study by Harrison [45] revealed the economic advantage of methane conversions at a higher pressure between 5-25 atm. Nevertheless, commercial relatively low-cost technologies were found to increase the metal oxide pressure to 6 bars [46], together with the thermodynamic constraints limiting the very high operating pressures for reduction step of thermochemical redox cycle.

In the present power plant, instead of combusting the natural gas, combustion of syngas in the form of partially oxidized methane has been proposed. Being an oxyfuel power plant, the combustion is done by near stoichiometric oxygen (5% excess) generated via a cryogenic ASU, that adds to considerable power penalty to the conventional NGCC. A part of the captured CO_2 is re-circulated back to the combustor to maintain the temperature of the outlet combustion gases into the turbine of the Gas turbine cycle.

The partial oxidation of methane in reduction reactor (RED) is highly endothermic, requiring around 50kW of heat per mol of Ce_2O_3 reduced. A large amount of heat has been proposed to be supplied by heat integration with the combustor of the gas turbine cycle as shown in Figure 3. An annular rector design is hence necessary whereby, the inner reactor would be the reduction reactor of the chemical looping unit, while the outer reactor would perform the work of the combustor. Such a reactor design, however, exist in literature, whereby detailed information on such reactor design concept can be obtained [47]. Modulating the quantity of CO_2 for recirculation within the reduction reactor, the net duty of the reduction reactor can be controlled, so as to provide the necessary heat required to drive the reduction reaction.

A part of the exhaust from the gas turbine has been proposed to be utilized for CO_2/H_2O splitting within the oxidation reactor (OXI) of the CL unit. A complete reaction would not only generate additional fuel in the form of syngas, that will then be utilized to produce additional power, adding to the system capacity further, but also oxidize the metal oxide back

to the higher valence state (CeO_2), that can then be recirculated back to the reduction reactor (RED) to continue the chemical looping cycle. However, auxiliary consumptions from compression for syngas and CO_2 for recycling would necessitate system optimization and identify suitable operating conditions. The oxidation reactions, as presented in equation (4) are essentially exothermic, which provides benefits of system control and improvement of efficiency by allowing generation of additional steam, as shown in Figure 3 (c). This would also simplify the recycling of the metal oxide between and RED and OXI reactors by eliminating the need of an additional heat exchanger for heating the oxidized metal oxide, and hence requiring lower heat duty for the reduction step. Higher the metal oxide temperature lower would be needed for supplementary heating. Therefore, an outlet temperature of around 1300-1400^{o}C from the oxidation reactor (OXI) would provide a significant advantage, requiring no intermediate heating needs for the oxidized metal oxide and increasing the mass flow of the exhaust gas due to higher recirculation of CO_2.

The exhaust gases from the gas turbines at elevated temperatures of over 800^{o}C would then be utilized for steam generation within the heat recovery steam generator (HRSG). Being an oxyfuel power plant and having natural gas as fuel, the impurities in the exhaust gas, especially SO_x, NO_x and particulates are negligible, allowing the gas to be cooled down to near ambient temperatures of around 50^{o}C, providing considerable advantages to the system efficiency, unlike traditional NGCC, where it is limited to about 140^{o}C to prevent acid condensation. Carbon capture methodologies are followed from traditional oxyfuel units, where, due to the high purity of the flue gas, simple water condensation leads to more than 99% pure CO_2. Besides the recirculated fraction of CO_2, the rest was sent for storage after compressing to a pressure of 110 bars.

In general, due to the addition of the CL unit, that recycles and utilizes a part of the exhaust gases within and for the system, a net improvement of the system efficiency has been envisaged. The novelty of this layout is, therefore, to improve the efficiency penalty through the addition of the CL unit to the conventional oxyfuel combined cycle with carbon capture while maintaining the same effectiveness of carbon capture by a typical oxyfuel unit of close to 100%.

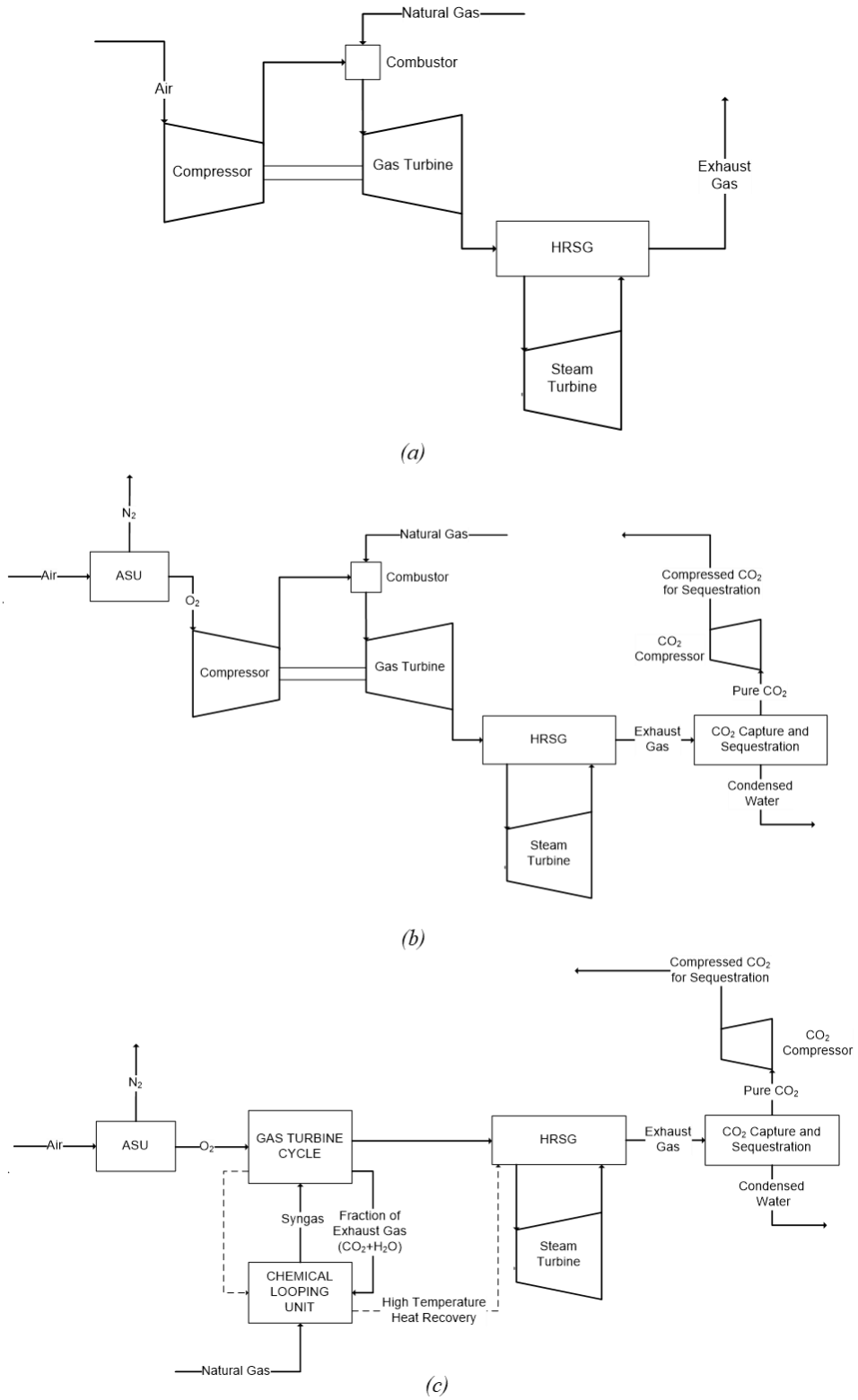

Figure 3 Block Diagram of NGCC, OXY-CC and the novel OXY-CC-CL process

4 Process Simulation and Assumptions

In this section, the detailed schematic of the conventional NGCC, OXY-CC and the proposed novel OXY-CC-CL are simulated using Aspen Plus® (v 8.8) and its corresponding existing functions and built-in modules. To predict the thermodynamic data and phase behaviour of a material stream, especially for systems for gas processing, it is recommended to use the PR-BM method which utilizes the Peng-Robinson cubic equation of state with the Bostone Mathias alpha function [48]. Therefore, in all the three processes, the PR-BM method was selected for the simulations.

The assumptions considered in the three processes based on Aspen Plus are summarized below:

- The heat losses in the reduction reactor (RED) and combustion process were neglected, while a pressure drop of 0.1 bar was considered in the combustion chambers (COMB1 and COMB2).
- A loss of 1% in the high-temperature gas lines were considered, especially for gases being transferred between components.
- The excess air number was considered as 1.05 for the oxy-combustion process.
- Equilibrium reactions have been considered in reduction (RED) and oxidation reactor (OXI), as well as the combustion chambers (COMB1 and COMB2), where the reaction residence time was long enough to achieve chemical and phase equilibrium.
- Steady-state simulations were performed, and the results hence obtained are not applicable to start-up or transient operations.
- Ambient temperature was assumed as 25^{o}C. Also, it was assumed to comprise 79% N_2 and 21%O_2 on a volume basis.
- Minimum approach temperature in heat exchangers was taken as 10^{o}C [48].
- The isentropic efficiency and mechanical efficiency for compressors and turbines were considered as 0.9 and 0.98, respectively. The pump efficiency was assumed to be 0.85 and 0.9, for isentropic and mechanical efficiency respectively.
- In actual scenario, natural gas instead of pure methane would be fed to reduction reactor (RED). Even though the purity of natural gas with respect to the sulphur content is considerably high, typical clean-up processes would be required. However, the removal of sulphur from the specific application was not considered within the

specific layout. Nevertheless, since no catalyst exists within the entire process, the purity on natural gas would not be a major concern, especially with respect to the operation of the CL unit.

- The primary objective of the present study is to recognize the potential efficiency gain from the combination of the chemical looping unit in a conventional oxyfuel plant, then the turbines and the HSRG were modelled as simple units, without reheating or multi-pressure systems. Indeed, by increasing the model complexity, the net efficiency can be gained considerably by process optimization for all the three cycles.

Moreover, design assumptions with respect to individual units of the NGCC, OXY-CC and OXY-CC-CL units, that were considered, have been shown in Table 1. Indeed, it has to be mentioned that the new system is not a retrofit, as it has been designed considering a separate entity, not being limited by parameters of a conventional NGCC.

Table 1 Design assumptions used for developing the process flowsheet models in Aspen plus

Unit	Applicable to	Parameters
ASU	OXY-CC and OXY-CC-CL	O_2 purity: 99.9% (by volume) ASU O2 and N_2 delivery pressure: 1.2 bars O_2 compression pressure: 26 bars for COMB-1 and 18 bars for COMB-2 No use of N_2 was considered
Turbo Expander	OXY-CC-CL	Feed Pressure of Natural Gas from OSBL: 70 bars Expansion Ratio: 35 Inlet Temperature of NG: 325^{o} C
Combustion Chamber	All	Excess Air factor: 182% Excess Oxygen factor: 5% Combustor Pressure Drop: 0.1 bar Combustor working pressure: 18 bars

Reduction Reactor (RED) and Combustion Chamber, COMB-1	OXY-CC-CL	Reactors were modelled separately with complete heat integration Working pressure: 26 bars in Combustor Side and 2 bars in Reducer Side Methane Conversion: 99%
Oxidation reactor (OXI)	OXY-CC-CL	Reactor Type: Adiabatic, jacketed for high-temperature steam generation Outlet Product Temperature: 1380^{o}C Working Pressure: 2 bars
CO_2 Drying and Compression	OXY-CC and OXY-CC-CL	Delivery pressure: 110 bars Delivery temperature: 40^{o}C Compressor isentropic efficiency: 90% Compressor mechanical efficiency: 98%
Gas Turbine/ Expander	All	Isentropic efficiency: 90% Maximum pressure ratio: 18:1 Discharge pressure: 1.04 bar Turbine inlet temperature (TIT): 1273^{o}C (1550K) for NGCC and Oxy-CL and 1373^{o}C (1650K) for Oxy-Cl-CC
Steam Turbine and HRSG	All	Single level pressure Turbine Isentropic efficiency: 90% IP Steam Pressure: 120 bars for NGCC and OXY-CC and 150 bars for OXY-CC-CL Condenser pressure: 0.04 bar Pump Isentropic Efficiency: 0.8 All of steam generated in gasification island, chemical looping and syngas cooling unit were expanded together Minimum Approach Temperature: 10^{o}C, no pressure drop

A detailed description of the OXY-CC-CL cycle as simulated within the ASPEN Plus environment is described as per depicted in Figure 4. Natural Gas (as per composition shown

in Table 2) is fed into the system at 20°C and 70 bar pressure from outside battery limit (OSBL) [49].

Table 2 NG Composition Assumed

Component	Value (% Mole Fraction)
Methane	94.00%
Ethane	4.20%
Propane	0.30%
CO_2	0.50%
N_2	1.00%
Total	100.00%

This natural gas is preheated with the syngas from the reduction reactor (Stream 4) before being expanded through a turbo-expander (TURBO-EXP) to the operating pressure of the chemical looping (CL) unit of 2 bars. The natural gas is then further pre-heated, where it is then fed to the reduction reactor (RED) at a temperature of approximately 890°C. The oxidized Ceria, in the form of Ceria (IV) Oxide, Ce_2O_3, (Stream 44), is fed at a temperature of 1375°C to the reduction reactor. Based on the thermodynamic results, the methane to ceria (CH_4/CeO_2) feed flow ratio of 0.7 is maintained for complete reduction of metallic ceria, to increase its effectiveness as an oxygen carrier. The heat of the reaction in the reduction reactor (RED) is provided directly by the heat of oxy-combustion of the syngas. The syngas, after exiting the reduction reactor at around 906°C, is used for methane heating, as well as, preheating of oxygen to around 140°C before entering the combustion chamber (COMB-1). The cooled syngas, compressed to 26 bars by COMP-1 is fed to the combustion chamber, COMB-1. The Combustion outlet temperature and hence the Turbine Inlet Temperature (TIT) is directly regulated by the flow of recycled CO_2, which, however, is also dependant on the heat needed to carry the reduction reactor forward in RED. The oxygen supplied for combustion is produced via a cryogenic air separation unit (ASU). A cryogenic pump was employed (O-PUMP) to increase the pressure of liquid oxygen, removing the need for an oxygen compression, thereby significantly reducing the plant auxiliary consumption.

Due to the ongoing technology development and considerable time being envisaged in future for such systems, as proposed to be practically employed, a turbine inlet temperature (TIT) of 1650K was assumed. To take advantage of the fact that the CL unit operates at a pressure of 2

bars, the turbine inlet pressure to the primary gas turbine was set at 26 bars to maximize the system outputs. The expanded gas (Stream-10) from the first gas turbine (GT1-1), around 1115^{o}C is split into two streams. One stream is fed to the oxidation reactor (OXI) for CO_2 and H_2O splitting to produce syngas as a fuel, while the remaining flue gas (Stream-12) is fed into the second gas turbine (GT1-2), where it is expanded to a near atmospheric pressure of 1.04 bar.

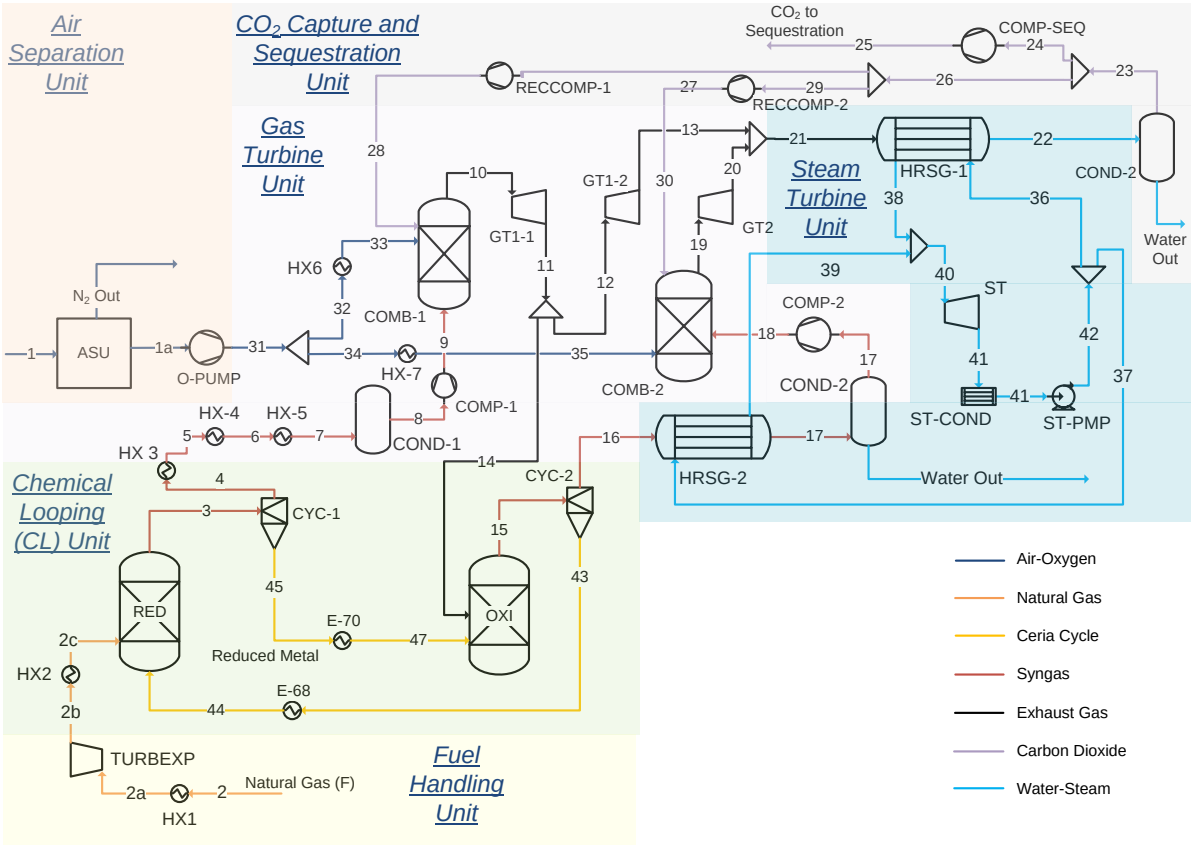

Figure 4 Process simulation flowsheet of OXY-CC-CL unit

The CO_2/H_2O splitting reactions are highly exothermic, and the metal oxide exit temperature is controlled via jacketed cooling. The product exit temperature of oxidation reactor (OXI) is set as being equal to the feed temperature of the reduction reactor (RED), which is around 1380^{o}C. The hot raw syngas at around 1380^{o}C from OXI (Stream-16) is cooled to around 50^{o}C in a heat recovery steam generation unit (HRSG-2). The cooled raw syngas is compressed to 18 bars (COMP-2) before being fed into the second combustion chamber (COMB-2) and subsequently into the Gas turbine at 1650K, 18 bars (Stream 19). The exhaust gases from the two combustion chambers (Streams 13 and 20) are then mixed and fed into the

HRSG (HRSG-1) for heat recovery steam generation by the downstream steam cycle. Being high purity gas, composed primarily of CO_2 and water, the gas was cooled down to near ambient temperatures of 50^oC. A live steam of 150 bars and 596^oC was generated for power production via the steam cycle from both the HRSGs Stream-38 and 39). The flow of steam was calculated accordingly. As mentioned, a simple single turbine Rankine cycle was modelled. The expanded steam at 0.4 bars is passed through a condenser (ST-COND) and pump (ST-PUMP) to subsequently complete the steam cycle.

The clean and cool exhaust gas from HRSG-1 (Stream-21), at 50 ^oC and 1.04 bar is fed into a flash chamber (COND-3), where the water is separated and almost 99% pure CO_2 is obtained. This CO_2 is therefore split into two streams. One stream (Stream-26) is further compressed and recycled back into the combustion chambers for temperature control as mentioned before. However, the other stream (Stream-24) is compressed to 110 bars by COMP-SEQ and sent for sequestration outside the battery limit of the designed power plant. Besides the discussed heat exchangers, no additional heat integration was considered. Indeed, a pinch analysis would be necessary thus to understand the heat availability in the unit and subsequently an improved design with better and improved location of heat exchangers can be developed in future.

The syngas composition exiting the two reactors of the chemical looping unit is shown in Table 3. The noticeable differences lie in the relative fraction of the H_2 and CO compositions of the two streams. While the H_2/CO ratio in the RED is 1.9, the corresponding value for the OXI is 0.16. Due to the supply of excess methane to the RED, the methane content in the outlet stream of the Reduction reactor is considerable. However, no methane is produced during the splitting reaction in the OXI. The content of water and CO_2 forms about 1.2% in the reduction reactor, while the corresponding value is higher in the OXI since excess reactants were passed to ensure complete reaction.

Table 3 Syngas composition from the Reduction Reactor (RED) and the Oxidation Reactor (OXI) of the Chemical Looping Unit

Mole Fraction (%)	From RED	FROM OXI
CO	28.43	61.4
H_2	54.23	9.84

CO_2	0.85	18.87
H_2O	0.35	9.63
CH_4	15.71	Trace
N_2	0.43	0.26
Total	100	100

5 System Performance Evaluations

5.1 Thermodynamic Performance

To obtain the comparative thermodynamic system performance of the proposed novel power plant with respect to the traditional power plants, the present analysis has been performed based on both the first and second laws of thermodynamics.

5.1.1 Energy Analysis

The energy analysis is based on the First Law of Thermodynamics and considers the principle of conservation of energy applied to a prescribed system. Assuming steady-state operations, together with kinetic and gravitational potential energies being negligible, the energy balance can be written as a rate equation [50]

$$0 = \dot{Q}_{CV} - \dot{W}_{CV} + \sum_{i} m_i h_i - \sum_{e} m_e h_e \quad (5)$$

Where $\dot{Q}_{CV}$ and $\dot{W}_{CV}$ are the specific heat required and work output from the selected control volume respectively, while the following two terms represent the net change in enthalpy of the between the outlet and the inlet streams of the same.

However, this simplified approach fails to provide appropriate system evaluation, especially concerning the correct evaluation of hest flows (in heat exchangers and other components where significant heat transfer is designed to occur).

5.1.2 Exergy Analysis

Exergy analysis or availability analysis, based on the second law of thermodynamics, is used to measure the maximum theoretical work. The exergy value, unlike the energy value of a stream, is based on its temperature, pressure and compositions as the stream passes from a given state to a state in equilibrium with the environment. Therefore, exegetic evaluation of

each material or energy stream is directly related to the assumed environmental state, which, in the present study was considered as $T_0 = 25^{o}C$ and $P_0 = 1atm$.

For steady state operations of an entire process, the total exergy destruction (Ex_{destr}) can be calculated via exergy balance as written by the following equation (7):

$$Ex_{destr} = Ex_{in} - Ex_{out} \quad (7)$$

where Ex represents exergy, the subscripts 'in' and 'out' representing the inlet and outlet, respectively. The overall inlet exergy of an NGCC or an oxyfuel NGCC cycle is derived directly from the exergy contained within the fuel (Ex_F). For the OXY-CC-CL plant, individual components like compressors, pumps, the energy required are derived directly from the energy generated within the system. As for heat needed for the reduction reactor of the CL unit, the system is designed to be self-sufficient due to the integration of the reduction reactor (RED) and the combustion chamber (COMB). Therefore, no additional external input is necessary for the proposed system in terms of exergy besides the fuel. The outlet exergy including the desired output in the form of electricity (W), material streams in the form of exhausted gas ($Ex_{exhaust}$) and available heat ($Ex_{Q,av}$), can be represented as per equation (8).

$$Ex_{out} = W + Ex_{exhaust} + Ex_{Q,av} \quad (8)$$

The un-used exergy of the system (Ex_{loss}) is defined as the sum of the amount of exergy destroyed (Ex_{destr}) and the amount of exergy wasted in the exhaust stream ($Ex_{exhaust}$) as shown in the following equation (9)

$$Ex_{loss} = Ex_{exhaust} + Ex_{destr} \quad (9)$$

A considerable amount of heat might also be available (based on system optimization and pinch analysis) from the proposed system, which adds benefits over the traditional NGCC or the oxyfuel unit $(Ex_{Q,ph})$. Hence, the net system output from the proposed OXY-CC-CL unit can be written as per the following equation (10)

$$Ex_{destr} = Ex_{in} - Ex_{out} \quad (10)$$

In general, the heat exergy is obtained as per the temperature of the available heat, given by the following equation (11).

$$Ex_Q = Q(1-(T/T_0)) \tag{11}$$

where Q is the amount of heat and T represents the temperature at which the heat is available. For a multicomponent material stream, the exergy (Ex_m) is often divided into three components of exergy, namely, the physical exergy (Ex_{ph}), chemical exergy (Ex_{ch}) and mixing exergy (Ex_{mix}) and written as per the following equation (12)

$$Ex_m = Ex_{ph} + Ex_{ch} + Ex_{mix} \tag{12}$$

The physical exergy is defined as the maximum work that can be extracted from a stream when it is made to pass from its current working conditions to the state of equilibrium with the environmental atmosphere [51,52]. The physical exergy is, therefore, dependent on the physical parameters, primarily temperature and pressure and can be calculated by Eq. (13), as obtained through the simulation results.

$$Ex_{ph} = (H-H_0) - T_0(S-S_0) \tag{13}$$

where H and H_0 are the enthalpy flow and S and S_0 are the entropy flow of a material stream at working and environmental state respectively.

Chemical exergy is defined as the maximum work which can be obtained when a substance is brought from the environmental state (physical equilibrium) in a state of further chemical equilibrium with the so named "dead state" by a reversible process which involves only heat transfer and exchange of substances with the environment [53]. The chemical exergy of pure components can be obtained from Bejan's reference environmental model [54], where the chemical exergy of a material stream is given by equation (14) as follows.

$$Ex_{ch} = F\left(y_{0,L}\sum_{i=1}^{n} y_{0,i} Ex_{ch,i}^{0L} + y_{0,V}\sum_{i=1}^{n} y_{0,i} Ex_{ch,i}^{0V} \right) \tag{14}$$

where F is the molar flow rate of a material stream, $y_{0,L}$ and $y_{0,V}$ denote the liquid and vapour mole fractions, respectively, $y_{0,i,L}$ and $y_{0,i,V}$ denote the mole fraction of component I in the liquid and vapour phases, respectively and denote the standard chemical exergy of component I in liquid and vapour phases, respectively.

The standard chemical exergies of pure solids, on the other hand, are mostly covered by the values provided by Kotas [55] and Szargut [51] in their respective works. Even though the standard chemical exergy of elementary Cerium (Ce) and CeO_2, as the most abundant form of ceria available in nature is available, the standard chemical exergy of Cerium (III) oxide

(Ce_2O_3) is not a reference subject in any readily available literature. However, it can be formed through the reaction of two moles of Ce and 1.5 moles of O_2 with known chemical exergies according to the reaction between Ce and O_2 as per the following equation (15)

$$2Ce + 1.5O_2 \rightarrow Ce_2O_3 \quad (15)$$

Subsequently, the chemical exergy of Ce_2O_3 can be calculated as per the following equation (16).

$$Ex^0_{ch,Ce_2O_3} = 2Ex^0_{ch,Ce} + 1.5Ex^0_{ch,O_2} + \Delta G^0_{Ce_2O_3} \quad (16)$$

where Ex^0_{ch,Ce_2O_3}, $Ex^0_{ch,Ce}$ and Ex^0_{ch,O_2} are the standard chemical exergy of Ce_2O_3, Ce and O_2, respectively; $\Delta G^0_{Ce_2O_3}$ represents the Gibbs free energy for the formation of Ce_2O_3 as per Ce/O_2 reaction shown in equation (15).

Finally, the mixing exergy, which always has a negative value, and can be estimated by equation (12) as per the following equation [48]

$$Ex_{mix} = \Delta H_{mix} - T_0 \Delta S_{mix} \quad (17)$$

where ΔH_{mix} and ΔS_{mix} are the enthalpy and entropy change due to mixing, respectively.

Hence, the common exergetic efficiency (η_{II}) of the power plants is given as the ratio of the useful exergy output from the system and the necessary exergy input to the process as follows from equation (18). On the other hand, the total exergy destruction from the individual components of the overall system is given as the summation of all the individual component exergy destruction as per equation (19).

$$\eta_{II} = \frac{W + Ex_{Q,av}}{Ex_F} \quad (18)$$

$$Ex_{destr} = \sum_i EX_{destr,i} \quad (19)$$

where $EX_{destr,i}$ refers to the exergy destruction of i^{th} component.

5.2 **Economic Performance**

To evaluate the economic performance of the proposed OXY-CC-CL unit, the most important economic parameters such as the capital cost (including specific investment costs), Operational and Maintenance (O&M) costs, levelized cost of electricity (LCOE) and levelized cost of CO_2 savings/avoided have been focused. In addition, not all the costs of all component were available up to date. In this regard, the costs would need to be updated for present day calculation. Chemical plant cost indexes were employed to transfer the literature values as per the present day values [56]. Also, a currency conversion factor of 1.23 USD/EUR was employed besides such considerations.

In order to determine the total Capital cost of the plant (CAPEX), the capital cost of each module or equipment is first estimated by utilization of the component scaling factor exponent, which is shown as the following equation

$$C_E = C_B \times (G / G_{ref})^M \quad (20)$$

where C_E and C_B represent the equipment cost with a capacity of G and G_{ref}, respectively; M being the equipment scaling factor exponent, varying between the range of 0.6 – 1, depending on the type of component [49,57]. The summary of the scale factors for the different components of the plant is presented in the following Table 3.

Table 4 Summary of the Different Plant Component Scale Factors [49,58–60]

Plant Component	Scale factor f
Gas turbine, generator and auxiliaries	1
HRSG, ducting and stack	0.67
Steam turbine, generator and auxiliaries,	0.67
Cooling Water System and Balance of Plant	0.67
CO_2 Compressor and Condenser - Compressor 1	0.67
Chemical Looping, Combustor and Oxy Reactor	1
Turbo Expander	0.67
Other Heat Exchangers	1

To assess further costs related to setting up of the power plant including installation and other direct and indirect costs related to the project development, a bottom-up approach following

the work of the CAESER project [49] was selected and is briefly described as follows and is shown in Table 4.

The *Total Equipment Cost (TEC)* is the sum of all module costs in the plant. Besides this, additional *installation costs* are incurred due to additional expenses required while integrating the individual modules into the entire plant, including costs for piping or valves, civil works, instrumentations, electrical installations, insulations, paintings, steel structures, erections and other outside battery limit (OSBL) activities.

Total Direct Plant Cost (TDPC) is then obtained as the sum of the Module/Equipment Costs and the Installation Costs. *Indirect Costs* have been fixed to 14% of the TDPC for all the three technologies [49], which include the costs for the yard improvement, service facilities and engineering costs as well as the building and sundries.

Engineering, Procurement and Construction Costs (EPC) was calculated as the sum of the Total Direct Plant Cost and Indirect Costs. Finally, the *Owner's Costs and Contingencies* (OCC) were included as the owner's costs for planning, designing and commissioning the plant and for working capital, together with contingencies, and were fixed to 15% of the total EPC cost for all the technology options as per literature [49]. In addition, the cost of initial metal oxide loading also adds an important consideration to the overall system CAPEX. Therefore, the overall CAPEX or *Total Plant Cost (TPC)* of the project could be obtained as per the following equation based on the explanation above.

$$\text{TPC} = \text{EC} + \text{Installation Costs} + \text{Indirect Costs} + \text{OCC} + \text{Metal Loading Costs} \quad (21)$$

In parallel, the O&M costs mainly comprise two aspects, namely fixed O&M costs and variable O&M costs. Fixed O&M costs comprise five components, i.e. general annual maintenance cost including overhead cost, property taxes and insurance and direct labour cost. On the other hand, variable costs are connected with the costs associated with power generation, include the cost of water (including both process water and make-up water), cost of a metal oxide for make-up, and fuel costs [49].

Table 5 presents the basic parameters used for calculating economic indicators of the proposed power plant including those discussed in the previous sections.

Table 5 Basic economic assumptions [49,61,62]

Item	Assumption
Natural gas price	0.04 $/kWh

Ceria oxide price	49 $/kg
Process Water	7.43 $/m^3
Make-up Water	0.43 $/m^3
Erection, Steel structures and Painting	49% of Equipment Cost
Instrumentation and Controls	9% of Equipment Cost
Piping	20% of Equipment Cost
Electrical Equipment and Materials	12% of Equipment Cost
Indirect Costs, including Yard Development, Building, etc.	14% of TDPC
Owner's Costs	5% of EPC
Contingencies	10% of EPC
Annual operational time	7450 hours
Property Taxes and Insurance	2% of TPC
Maintenance Cost	2.5% of TPC
Labour Cost (Million Euro)	$100 per kW
Operational Life of Plant	30 years
Discount Factor	10%
Carbon Credits	None of the base case evaluation
Electricity Price	58.3 $/MWh

The levelized cost of electricity (LCOE) provides the "break-even" value for producing a unit of electricity, often employed as a parameter to compare different electricity production technologies from the economic point of view. The LCOE is expressed as the following expression (equation 22), based on the investment cost at time period t (I_t), O&M Costs at time period t (M_t), Fuel Cost at time period t (F_t), the electricity generated at time t (E_t) and the interest rate r.

$$\mathrm{LCOE} = \frac{\sum \frac{I_t + M_t + F_t}{(1+r)^t}}{\sum \frac{E_t}{(1+r)^t}} \tag{22}$$

The levelized cost of CO_2 capture (LCOA), on the other hand, is calculated based on the corresponding formula as presented by the equation (23). The calculation is based on the

discounted expenses of operating the power plant including the investment costs with respect to the emissions saved in comparison to a conventional NGCC.

$$\mathrm{LCOA} = \frac{\sum \frac{I_t + M_t + F_t}{(1+r)^t}}{(CO_2\text{abated} / \text{yr}) \times t} \tag{23}$$

5.3 Environmental Performance

The environmental performance of the OXY-CC-CL in comparison with the conventional NGCC and the oxyfuel combustion units was evaluated based on multiple criteria. The fundamental criteria selected were the CO_2 savings. Indeed, this forms the single most interesting criterion for such assessments. However, other criteria were studied to observe the broader picture with respect to the sustainability of a technology.

Water availability will become a critical issue in future and especially for plants with carbon capture [63]. In this regard, an analysis of the water requirement with respect to conventional technologies was evaluated after the method proposed by Martin, 2012 [64]. The specific water needs (I) for the present system in terms of litre/kWh was calculated based on the following equation (24) accounting for the water needed for both cooling and process applications [64]. An assumption of employing wet cooling tower was considered and corresponding values were selected from the literature.

$$I = A \times (HR - B) + C \tag{24}$$

Where A is a constant depending on the type of cooling = $5.03*10^{-4}$ litre/kJ based on wet cooling [64]; HR represents the heating rate and B represents the net output of the system, both with respect to useful energy in electricity or heat and system losses. Hence, (HR-B) represents the amount of cooling load necessary. C represents the process water needed by the system other than the cooling system. It is to be noted that the Chemical looping unit demands no additional water beside cooling. Therefore, the water need for a conventional NGCC with CCS remains constant also in this case = 0.2 Litre/kWh [64].

Land footprint assessment is another additional sustainability criterion, important to analyse the system viability. Indeed, additional systems with increased system complexity would increase the need for space required to accommodate additional units. Florin and Fennel [65] proposed an alternative to the linear model of spatial footprint assessment due to its over-

simplistic approach leading to inaccurate evaluations. A suggestion was made to take a modular approach and scale footprint with respect to the number of capture trains. Berghout et al [60] proposed to evaluate the capacity increase of process equipment as the third power of the size (determined by volume) while the capital costs would increase in a quadratic way (based on the surface area). Therefore, the spatial footprint of the capture components for plant scale k (m^2) was assessed as follows from the following equation 25.

$$A_k = \sum_i [A_{i,ref} \times (\frac{S_i}{S_{i,ref}})^{SF_i}] \quad (25)$$

where $A_{i,ref}$ represents the space requirement for component i for the reference capacity (m^2), S_i refers to the capacity of component i for plant scale k (unit as per the component), $S_{i,ref}$ being the reference capacity of component i for plant scale k (unit as per the component), and SF_i refers the scaling factor for component i. As per Berghout et al [60], a scaling factor of 0.67 (or 2/3) was used. An additional 20% margin was added to the computed physical footprints considering space requirements for installation and maintenance.

6 Thermodynamic Evaluation of the OXY-CC-CL Unit.

6.1 Energy Analysis of OXY-CC-CL

Table 6 lists the detailed technical assessment results for the proposed OXY-CC-CL power plant. The results are expressed in terms of power generation from gas and steam turbines, overall plant thermal efficiency, total energy penalty, net CO_2 emission savings and relative efficiency gain.

Table 6. Global Energy Flow and Energetic Efficiency of the Proposed OXY-CC-CL Unit

Plant data	Units	OXY-CC-CL
Fuel Energy Input, LHV (A)	MWth	990.708
Net GT Output	MWe	484.233
GT Output from CO_2 recycling	MWe	110.039
ST Output	MWe	255.937
Gross Electric Power Output (B)	MWe	750.206
ASU Consumption + O_2 compression	MWe	63.383

CO_2 Capture and Compression	MWe	19.222
Power Cycle Pumps	MWe	3.287
Air/ Recycled CO_2 Compression	MWe	142.879
Syngas Compressors	MWe	17.188
Total Parasitic Power Consumption (C)	MWe	245.959
Net Electrical Power Output (D=B-C)	MWe	504.247
Gross Electrical Efficiency (B/A*100)	%	75.72%
Net Electrical Efficiency (D/A*100)	%	50.7%
CO_2 Capture Efficiency	%	100%
CO_2 captured	t/h	178.658
Electric Power Output per tonne of CO_2 Captured	MWh/t	2.822

As can be observed from Table 6 a considerable share of the generated electrical energy is used up for oxygen separation in the ASU and also for recycling the carbon dioxide for being fed into the combustion chamber for temperature control. Some fraction, around 3.8% is also used for compressing the captured CO_2. The extra energy needed for carbon capture and storage is known as the energy penalty with respect to the conventional base case NGCC without carbon capture. These, in addition to the auxiliary power requirement, become the two major penalties for the conversion of energy from the chemical energy of natural gas to electricity. However, generation of around 110 MW of electricity from the recycling of the waste gas through splitting of CO_2 and H_2O in the oxidation reactor (OXI) to produce syngas results in considerable improvement of the net power output, even with almost 100% Carbon Capture. An impressive energy efficiency of 50.7% with carbon capture is obtained. This correspondingly aids the lowering of the net energy penalty due to CCS in a conventional oxyfuel NGCC. Additionally, generation of heat by integration of the power plant units might result in energy savings and decrease the overall penalty by working the power plant on a combined heat and power mode.

6.2 **Exergy Analysis of OXY-CC-CL**

The exergy flow of the proposed OXY-CC-CL unit is depicted in Table 7. As can be clearly observed, due to both electricity and heat self-sufficiency of the system, the input fuel, namely natural gas contributes entirely (100% of the total exergy input) to the net exergy input to the system. The work consumed for compressors and pumps comprise a relatively

small contribution to the entire input exergy (4.83%). However, the ASU alone would consume around 3.04% of the net input exergy of the entire system.

The exergy consumed for capturing CO_2 represents a large fraction of the total exergy input (7.27%), which includes the net exergy destruction related to water condensation and compressing the CO_2 to 110 bars for the sequestration.

On the other hand, the majority of the system output is electricity (393.75 kJ/mol of CH_4). The exergy exhausted in gas contributes 24.4% of the process inlet exergy. Approximately 28.5% of the exergy was destroyed due to irreversibility within the system. Indeed, the system optimization would considerably improve upon the net exergy destroyed by decreasing the unused fraction of exergy amounting to 52.9% of the net input exergy.

Table 7. Global Exergy Flow and Efficiency of the OXY-CC-CL unit

	Exergy (kJ/mol CH_4)	% of total Ex_{in}
Net Exergy into the Plant	835.34	100
Exergy in Methane	835.34	100
$W_{compressors}$	40.31	4.83
W_{pump}	0.23	0.03
W_{ASU}	25.43	3.04
CO2 Capture including CO2 compression	60.73	7.27
Exergy Out	597.66	71.55
Exhausted gas	203.92	24.41
Exergy destroyed	237.68	28.45
Exergy un-used	441.59	52.86
Exergy efficiency (4)	393.75	47.14

To evaluate the primary reasons of exergy destruction caused in the simulated OXY-CC-CL process, an exergy analysis of each component was performed, as listed in Table 8. The methane preheating, occurring between HX-1 and HX-3 before the turbo-expander and HX-2 and HX-4 (hot side and cold side respectively) after the turboexpander is referred to as FPH-1 and FPH-2 respectively as two separate heat exchangers. Also, for physical processes occurring in heat exchangers, pumps, compressors, etc., the chemical exergy is not involved in the energy transformation process, and the component exergy efficiency $\eta_{II,comp}$ can be

predicted by equation (18). The final column depicts the relative irreversibility of each component with respect to the net irreversibility of the entire process, that is, reports the component exergy destruction percentage ($Ex_{destr,i}$) with respect to the total exergy destruction (Ex_{destr}).

Clearly, compressors (COMP-1, COMP-2 and RECCOMP 1 and 2) and pump work represent a minor fraction of total Ex_{destr}. Turbines, heat exchangers and the reactors contribute a higher percentage of exergy destruction. The heat exchangers contribute 21.27% of Ex_{destr}, which are inherently destroyed exergy due to the heat transfer across a finite temperature difference [66]. However, the mixture, from the mixing of the two gases from turbine outlets plays the most significant role in the net exergy destruction of the proposed power plant, contributing to over 37% of the same.

A significantly high exergetic efficiency can be observed in the combustion chamber due to oxyfuel combustion and also the assumptions of no heat losses. The CO_2 separation unit in the form of the water separator and corresponding CO_2 compression contributes to a significant fraction of the total exergy losses, accounting for over 8% of the total Ex_{destr}.

Therefore, as can be observed from the exergy analysis of each of the component of the OXY-CC-CL a better integration of the entire power plant through design optimization would lead to a considerable decrease in exergy losses.

Table 8. Exergy balance in OXY-CC-CL break-down by component

Type	Component	$Ex_{in,i}$(MW)	$Ex_{out,i}$(MW)	Ex_{dest},(MW)	Component η_{II} (%)	Ex_{destr} % of Total
Physical process	**FPH-1**	2043.98	2031.8	22.47	99.404	1.33
	TURBEXP	1082.35	1078.34	12.18	99.629	0.438
	FPH-2	2138.06	2089.36	4.01	97.722	5.314
	CMP-1	976.05	975.76	48.7	99.97	0.031
	RECCOMP-1	323.83	303.55	0.29	93.735	2.214
	GT1-1	1007.57	932.69	63.05	92.569	8.17

	GT1-2	859.54	848.36	74.87	98.699	1.221
	HRSG-2	292.64	254.88	36.59	87.098	4.12
	COMP-2	222.67	221.8	37.76	99.612	0.094
	RECCOMP-2	125.54	95.38	0.86	75.971	3.292
	GT2	319.38	287.27	3.17	89.945	3.504
	HRSG-1	628.37	547.73	343.82	87.166	8.801
	ST-COND	25.78	9.63	80.65	37.373	1.762
	ST-PUMP	12.9	12.6	16.14	97.698	0.032
	COND-3	351.95	301.19	0.3	85.579	5.539
	COMPSEQ	73.87	46.87	50.76	63.447	2.947
Physical and Chemical Processes	**ASU**	63.19	40.73		64.447	2.452
	RED & COMB-1	2653.46	2590.42	20.29	97.624	6.88
	OXI	561.58	524.99	11.18	93.484	3.993
	COMB-2	322.55	319.38	30.17	99.018	0.346
	Mixture	960.75	616.93	32.11	64.213	37.52
	Total	1069.55	501.65	27	7	100

6.3 Effect of key operating parameters

The impact of key process variables, viz., temperature, pressure, system size, etc. on the process performance characteristics of the OXY-CC-CL process was systematically examined through a comprehensive series of simulations using the proposed power plant integration scheme. The variation of the outputs from the gas turbines, the steam turbine, the net power output and the system efficiency have primarily been analysed. Results of these analyses are presented in this section from Figure 5 through Figure 8.

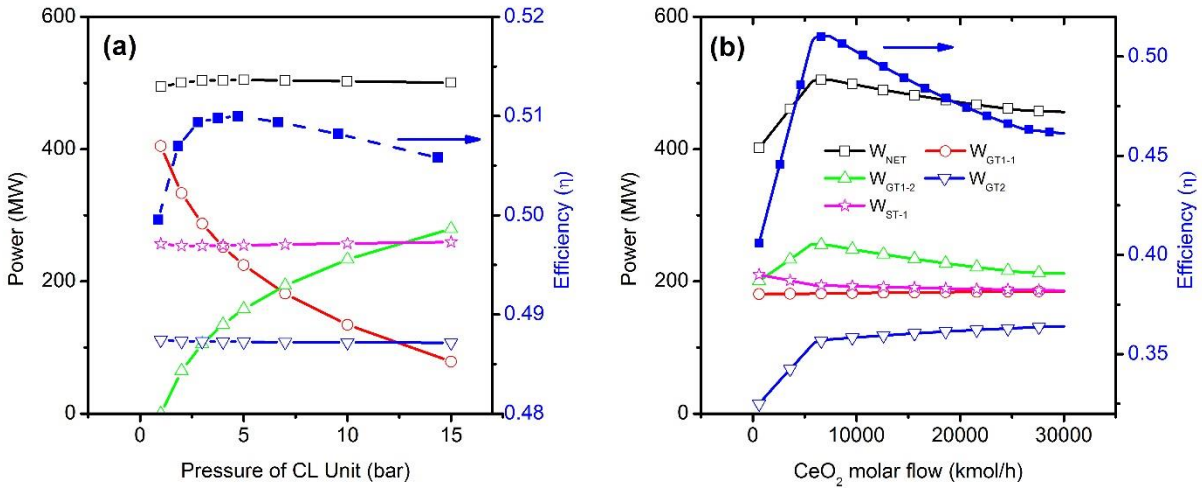

Figure 5. Impact of the variation of a) pressure of the CL unit and b) molar flow rate of Cerium Oxide (CeO_2) at a constant natural gas flow and on the power generating components, the net power produced and the efficiency of the OXY-CC-CL power plant.

Figure 5(a) represents the effect of operating pressure of the CL unit on the defined parameters. A minimal rise in the net power output from the entire plant is observed with increase of pressure in the CL unit. While there is a proportional increase and decrease of the power output from GT1-1 and GT1-2 respectively, due to varying pressure ratios, the power outputs from the steam turbine and that of WGT2 remains constant. However, at a pressure of 1 bar, the compression ratio of the produced syngas from the CL unit for power generation is the highest, 22, leading to the efficiency recorded as lower than 50%. Indeed, with a rise in the operating pressure of the CL unit, the compressor work for syngas compression decreases considerably. However, beyond 5 bars, the conversion of methane in the reduction reactor drops, together with a slight decrease in compression ratio of syngas and a low power output from the turbo-expander. These factors combined lead to a drop in the efficiency of the power plant beyond 5 bars to around 50.5% at 15 bars operation pressure of the CL unit.

The performance study of the system with respect to the variation of the circulating metal oxide indicated similar trends in efficiency of the plant. At lower CeO_2 flowrates in the CL unit, the combustion in the COMB-1 is with natural gas, since no partial oxidation takes place in the reduction reactor (RED). All other parameters remaining constant, this results in a power output similar to traditional OXY-CC, and hence a corresponding low efficiency. However, with higher CeO_2 flow in the CL unit, the production of syngas in the OXI and subsequent power production through exhaust gas recycling increases not only the efficiency,

but also the net power output of the system. However, with higher CeO_2 flow rates, and therefore, with correspondingly higher fraction of exhaust being sent to the OXI, the net yield from WGT1-2 decreases, with no net increase in the efficiency. This leads to a drop in efficiency at very high CeO_2 flow rates (5 times the CH_4/CeO_2 stoichiometry for metal oxide reduction) to as low as 46%. Interestingly, the highest efficiency, around 51% occurs at a CH_4/CeO_2 stoichiometric ratio of around 0.8.

The variation of fraction of exhaust gas (mixture of CO_2 and H_2O) from the WGT1-1 to the oxidation reactor (OXI) for syngas production through splitting was investigated. It was observed that a peak system efficiency of 50.7% occurs at a split fraction of 0.1. At lower split fractions, the net utilization of the circulating CeO_2 is low, thereby producing low syngas for power production in WGT2. However, a higher split fraction, even though increases the power generated from WGT2, lowers the power output from WGT1-2 nonetheless, while simultaneously increasing the auxiliary power consumption of COMP-2. This results in the net efficiency to be lowered to around 48.5% with 25% recycling of exhaust gas to the oxidation reactor as seen in Figure 6(a).

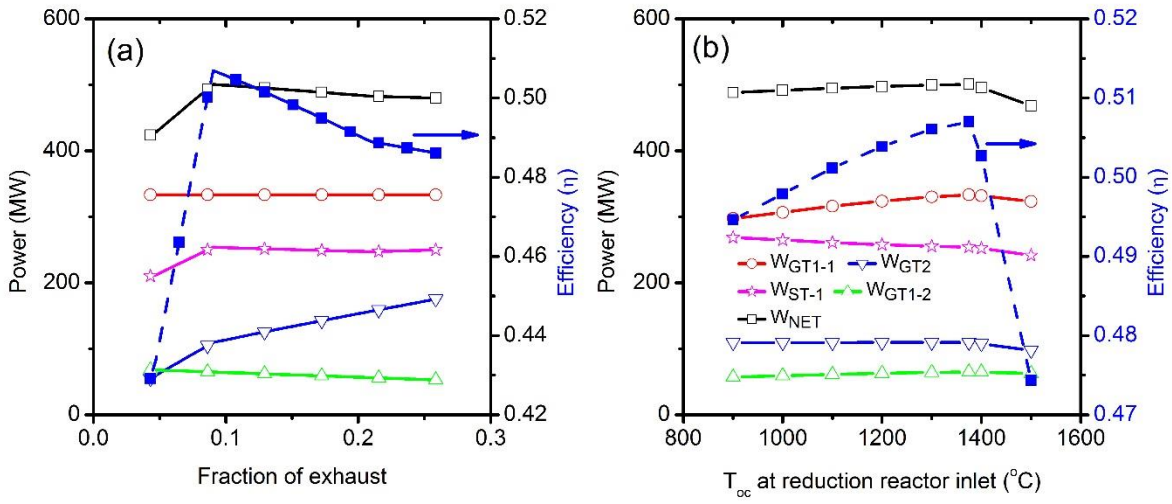

Figure 6. Impact of the variation of a) fraction of the exhaust gas from GT1-1 recirculated into the oxidation reactor (OXI) of the CL unit for production of syngas and b) temperature of the CeO_2 at the inlet of the reduction reactor (RED) of the CL unit at constant natural gas flow on the power generating components, the net power produced and the efficiency of the OXY-CC-CL power plant.

The temperature of the CeO_2 (oxygen carrier) inlet to the reduction reactor (T_{oc}) has a significant impact on the system efficiency as shown in Figure 6 (b). An optimal value of about 50.7% is reached at a temperature of around 1375^{o}C. This is directly related to the fact that the endothermicity of the reaction needs to be maintained through variation of the recycled CO_2 in the combustor (COMB-1). This is due to the fact, that with higher oxygen carrier temperature, the endothermicity of the reaction (equation (3)) drops, requiring more carbon dioxide to be recycled to the combustor to maintain the TIT to its desired level. Consequently, an increase in the GT1-1 output power is noticed, however, beyond 1375^{o}C, a steep drop in the system efficiency is observed. Due to an increased reaction endothermicity, the system performance is adversely affected, both with respect to the power produced and auxiliary consumptions. Therefore, an efficiency, as low as around 47.5% is obtained at a T_{oc} of 1500^{o}C.

The variation of the Turbine inlet pressure of the Gas turbines was also studied. Commercial scale stationary gas turbines are usually limited to a working pressure ratio of 18:1 [67]. Considering an operation pressure of the CL unit of 2 bars, the inlet pressure of GT1-1 was varied between 15 bars and 30 bars. As can be seen from Figure 7(a), the inlet pressure primarily increases the power output from GT1-1, and therefore, the net system power output, and the efficiency. However, it correspondingly also increases the compression ratio of COMP-1, lowering the net benefit of increased power output to some extent. At a turbine inlet pressure of GT1-1 of 30 bars (pressure ratio 15) an efficiency of 51.2% was obtained.

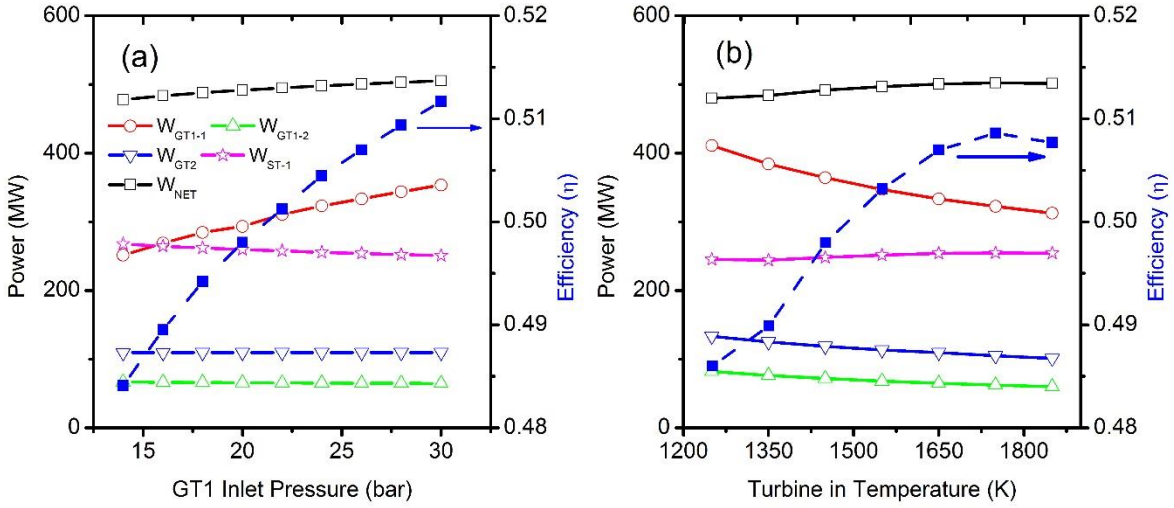

Figure 7. Impact of the variation of a) GT1-1 inlet pressure and b) Turbine Inlet Temperature (TIT) for both the turbines (GT1-1 and GT2) at constant natural gas flow on the power generating components, the net power produced and the efficiency of the OXY-CC-CL power plant.

Turbine Inlet Temperature (TIT) of the gas turbines critically impacts the system efficiency. All the gas turbines have been assumed to be kept at the same TIT. A lower TIT results in a lower efficiency, more specifically, around 48.5% at 1250K, which is subsequently improved to around 51% for a TIT of 1750K as shown in Figure 7(b). Hence, the efficiency of the OXY-CC-CL unit, proposed for operation at 1650K TIT, can be increased further. Interesting to note, that even if the absolute power output from the individual turbines, besides the steam turbine, decreases, the net power output and the efficiency increases. This can be explained by the fact, with a higher TIT the CO_2 recycled into the combustion chambers (COMB-1 and COMB-2) decreases, thereby considerably improving the overall power output from the system. However, at temperatures beyond 1750K, the power output from the all the gas turbines (GT1-1, GT1-2 and GT2) decreases, with subsequently lower gain from decreased CO_2 compression. This results in a drop of efficiency to about 50.75% at a TIT of 1850K.

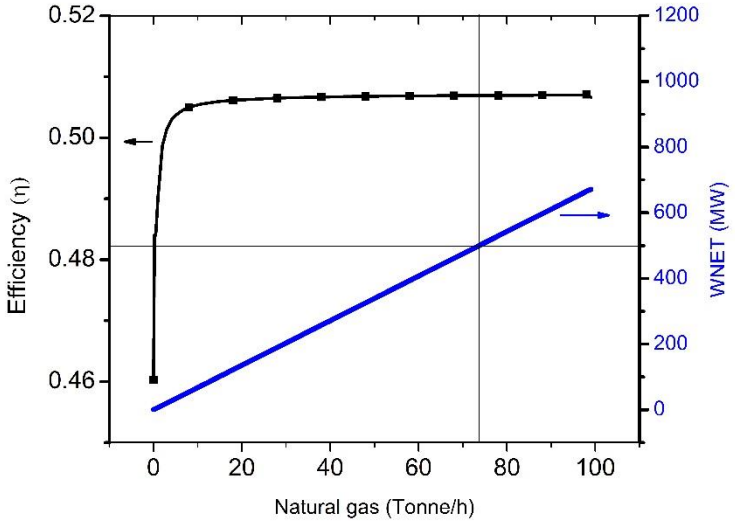

Figure 8. Impact of the variation of natural gas flow rate on the system capacity (net power produced) and the efficiency of the OXY-CC-CL power plant

Finally, the impact of scale on the system efficiency is depicted in Figure 8. For a 500MW power plant, the efficiency obtained was 50.7% corresponding to a natural gas flow rate of 73.75 tonnes per hour. Indeed, the impact of the scale was obtained to be limited towards the net system efficiency till around 10 MW. As can be seen, the efficiency of the system above 10 MW is constant around 50.7%. However, below such size, the efficiency drops significantly to about 46% for a size of 1MW, limiting downsizing of such systems beyond certain limits as shown in Figure 8.

7 Comparative Performance Evaluation of State of the Art NGCC, Oxyfuel NGCC with Carbon Capture and OXY-CC-CL unit.

7.1 Thermodynamic Performance

The performance of the NGCC, OXY-CC and OXY-CC-CL plants are compared on the basis of net electrical efficiency and CO_2 emissions for thermodynamic evaluation. Detailed simulation results for both cases are summarised in Table 9. The base case, without any CO_2 capture, emits 178.65 t/h of CO_2. In contrast, both the OXY-CC and the OXY-CC-CL with CO_2 capture does not emit any significant quantity of CO2, leading to near 100% capture of CO_2. As per the developed ASPEN plus model, the non-optimized base case NGCC has an efficiency of 54.65%, agreeable to efficiencies of state of the art NGCC, as available in the

literature [29,68]. However, this considerably drops due to the addition of the ASU and CO_2 sequestration compressor for the OXY-CC power plant, which has a much lower efficiency of 43.25%. Therefore, an efficiency penalty of more than 11 percentage points can be seen. Indeed, as predicted with the above analysis, the novel OXY-CC-CL unit, with an efficiency of 50.7% was able to improve the efficiency of the power plant by around 7.5 percent points due to internal recycling of a part of the exhaust gases that can be termed as CO_2 recycling. This also decreases the corresponding total parasitic load of the power plant due to a relative increase in the net work output from the proposed unit.

Table 9. Plant performance indicators for State of the Art NGCC, oxy-fuel NGCC, and the oxyfuel NGCC with CL unit (OXY-CC-CL) processes obtained by Aspen plus simulations

Plant data	**Units**	**NGCC**	**OXY-CC**	**OXY-CC-CL**
Fuel Energy Input, LHV (A)	MWth	910.764	1155.267	990.708
Net GT Output	MWe	693.332	570.372	484.233
ST Output	MWe	160.400	259.042	255.937
Gross Electric Power Output (B)	MWe	853.732	829.414	750.206
ASU Consumption + O2 compression	MWe		113.507	63.383
CO_2 Capture and Compression	MWe		26.523	19.222
Power Cycle Pumps	MWe	1.880	3.067	3.287
Air/ Recycled CO_2 Compression	MWe	351.759	186.664	142.879
Syngas Compressors	MWe			17.188
Total Parasitic Power Consumption (C)	MWe	353.639	329.762	245.959
Net Electrical Power Output (D=B-C)	MWe	500.093	499.652	504.247
Gross Electrical Efficiency (B/A*100)	%	93.74%	71.79%	75.72%
Net Electrical Efficiency (D/A*100)	%	54.91%	43.25%	50.70%
CO_2 Capture Efficiency	%		100%	100%
CO_2 Emissions	t/h	178.658		
CO_2 specific Emissions	t/MWh	0.505		

Figure 9 shows the relation between power produced and consumed in different units for three cases studied. The net power output from the three cases was kept constant to develop a comparative evaluation. The net thermal energy input from the natural gas, is, however, different in the three different cases resulting in the variation of the net energy efficiency

from the three units. In the base case NGCC, the overall heat is completely produced in a single combustion chamber, whereby, the natural gas is combusted with an excess of air in the combustion chamber, the exhaust gases of which being first fed into the gas turbine for electricity generation and then in HRSG for heat recovery. Similar to this, OXY-CC also combusts the natural gas in a single step, however, with 5% excess of oxygen and recycled CO_2, reducing the power output by 77 MW. Unlike to the previous two cases, a mixture of CO, H_2 and CH_4 is burned in 5% excess oxygen and over 90% recycled CO_2, lowering further the net power output from the gas turbine. Indeed, for the OXY-CC-CL, the net power output from the gas turbines include two-step expansion, one from 26 bars to 2 bars and subsequently up to 1.04 bar after exhaust gas separation for splitting, together with the gas turbine output from the split exhaust gas containing syngas. This lowers the contribution from the gas turbine, however, increasing the contribution from the steam cycle, comparable to that of OXY-CC unit. Nevertheless, the gross power of the OXY-CC-CL unit is significantly lower by around 100 MW from the base NGCC and 80 MW from the OXY-CC power plant. However, interestingly, the parasitic load of the proposed OXY-CC-CL unit decreases by more than 105 MW and 85 MW respectively than base NGCC and OXY-CC unit, thereby showing better energetic performance than the traditional OXY-CC system.

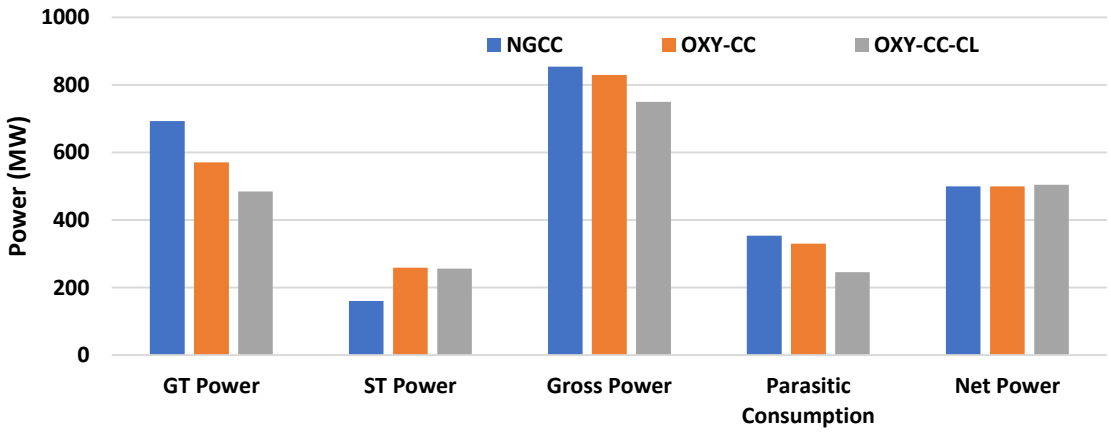

Figure 9. Comparison between GT, ST, gross, parasitic and net power output for base NGCC, OXY-CC and OXY-CC-CL

Table 10 depicts the comparative energy and efficiency penalty associated with CO_2 capture between the reference base case NGCC, OXY-CC and the proposed novel OXY-CC-CL unit. As can be seen from Table 10, the relative decrease in net electrical efficiency from the

NGCC and the OXY-CC and the OXY-CC-CL units is around 11.4% and 4% respectively. Therefore the proposed new system performs better than Oxyfuel-CC with carbon capture as reported in the CAESER project [49]. The CO_2 captured per MWh of energy expended in the OXY-CC-CL (11.34 t/MWh) is therefore significantly higher than the corresponding energy expended for CO_2 capture in the OXY-CC process (4.35 t/MWh). These results suggest that OXY-CC-CL unit is a more favourable option from the energetic point of view (without economic considerations) to capture CO_2 from NGCC power plants compared to simple Oxyfuel unit. Indeed, a much lower relative decrease, by about 14 percentage points, with respect to the base case NGCC makes the proposed technology highly interesting for future NGCC power plants with CCS, especially while striving for higher efficiencies. However, the OXY-CC power plant is a practically proven and commercially available technology, while the OXY-CC-CL unit requires considerable further research and optimization to be available for commercial use.

Table 10. CO_2 Captured per unit energy and efficiency penalty with reference to conventional Oxyfuel NG Power Plant

Plant data	**Units**	**NGCC**	**Oxyfuel-CC with CCS**	**OXY-CC-CL with CCS**
Energy Penalty (A)	MW		57.635	18.453
CO_2 Captured (B)	t/h		251.014	209.3
CO_2 captured per MW decrease in energy Production than Base Case NGCC (C=B/A)	t/MWh		4.3553	11.3422
Net Electrical Efficiency (D)	%	54.91%	43.25%	50.7%
Net Electrical Efficiency Penalty Compared to Base Case NGCC, E=(54.65-D)	%		11.52%	3.69%
Relative Decrease in Net Electrical Efficiency Compared to Base NGCC F=E*100/54.65	%		21.089%	6.752%
CO_2 Captured per unit decrease in net	t		21.780	56.721

electrical efficiency from Base Case NGCC (B/E)

8 Economic Analysis

8.1 Capital Cost and Operational Expenses

As developed from the process simulations, it can be easily concluded that the OXY-CC-CL unit has a clear technical edge over conventional and advanced NGCC system with and without carbon capture. However, for integration purposes, the OXY-CC-CL unit needs considerable new system additions including solid handling units, reactors for reduction and oxidation, an additional combustion chamber among others. This would incur additional capital investments. Therefore, an economic analysis was performed to find the economic feasibility of the proposed OXY-CC-CL systems and is presented in detail in this section.

Table 11. Capital Cost Breakdown of the proposed OXY-CC-CL unit

Plant Component	Values (million $)	% Contribution
Primary Gas turbine, generator and auxiliaries	76.09	6.20%
Primary Low-Pressure Gas turbine, generator and auxiliaries	14.79	1.20%
Secondary Gas turbine, generator and auxiliaries	25.1	2.05%
HRSG, ducting and stack	21.39	1.74%
Steam turbine, generator and auxiliaries,	49.76	4.05%
Cooling Water System and Balance of Plant	63.26	5.15%
CO2 Compressor and Condenser - Compressor 1	16.27	1.33%
Chemical Looping, Combustor and Oxy Reactor	48.72	3.97%
Turbo Expander	2.93	0.24%
Other Heat Exchangers	1.73	0.14%
Total Equipment Costs (TEC)	320.04	26.07%
Cost of Metal Loading	0.01	0.00%
Total Installation Costs	309.1	25.18%
Total Direct Plant Cost (TDPC)	624.48	50.87%

Indirect Costs	87.43	7.12%
Engineering Procurement and Construction Costs (EPC)	711.91	57.99%
Owner's Costs	8.74	0.71%
Contingencies	71.19	5.80%
ASU (Complete CAPEX as an add-on unit)	435.7	35.49%
Total Project Costs (TPC)	1,227.55	100.00%

Table 11 represents the cost breakdown of the proposed OXY-CC-CL unit. The ASU was assumed as an add-on unit, with a CAPEX of $435.70 million, contributing to about 35.5% of the entire plant cost. The net project CAPEX was obtained at around $1227 million, which amounts to around 2455 $/kW, a relatively high cost than the present day NGCC power plants without carbon capture, with overnight capital costs reported as 978 $/kW [69]. On the other hand, the capital costs become comparable to advanced NGCC with carbon capture, quoted around 2050 $/kW as per the 2016 study by the US Department of Energy [70].

In addition, the operational expenses were calculated based on the assumptions mentioned in the earlier section. The net fixed OPEX was obtained as $62.58 million, while the variable cost was calculated as 50.15 $/MWh of gross power generation. Hence a net annual operating cost of $347.1 million was calculated to run the proposed 500 MW OXY-CC-CL unit.

8.2 LCOE and LCOA Calculations

LCOE calculations were hence developed based on equation (22) with assumptions listed in Table 5 to perform a comparative evaluation of the system economic performance. As mentioned, no carbon tax was assumed. Correspondingly an LCOE of 128.01 $/MWh was obtained. However, as depicted in Figure 10, with a carbon credit of 6 $/tonne CO_2, the LCOE would drop to comparable prices of the average wholesale electricity market prices [71]. Therefore, the importance of Carbon Credits for such systems to be economically competitive is most crucial.

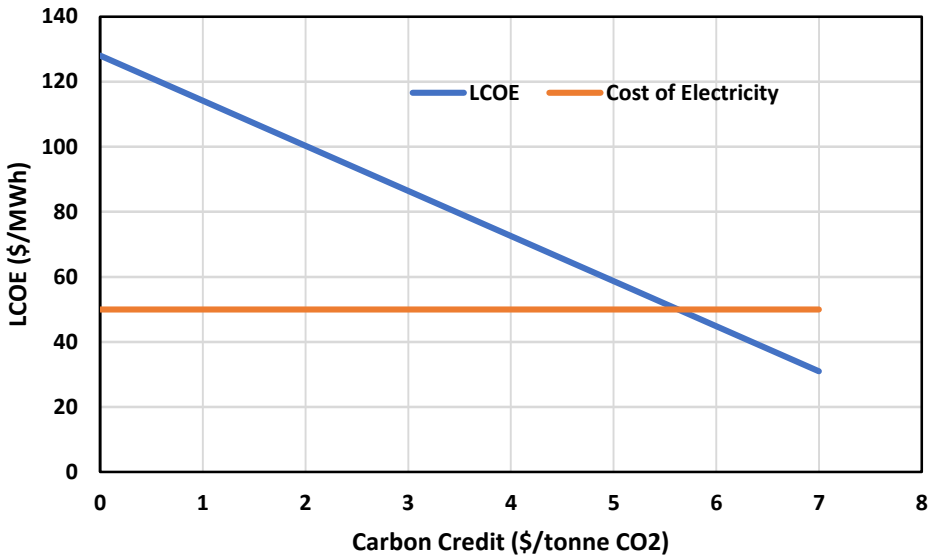

Figure 10. Impact of Carbon Tax on the Levelized Cost of Electricity of the proposed OXY-CC-CL unit

Additionally, levelized cost of CO_2 savings (LCOA) was calculated to obtain the economic performance of carbon capture. Indeed, as can be seen in Figure 11, the levelized cost of carbon capture for the proposed OXY-CC compares well to those of already available technologies. Indeed, with an LCOA of 96.25 $/tonne of CO2, the cost is lower than that of the oxyfuel power plant with carbon capture, reported as 104 $/tonne of CO2 by Khorshidi et al., 2012 [72]. A higher efficiency, lowering the need for fuel consumption for similar power production is a considerable benefit. As for post-combustion capture, the value is on the higher side, being needed to be integrated for a new and much complicated power plant, increasing the costs. Also for the OXY-CC power plant, a LCOA of 104 $/tonne CO2 captured was reported by the study by Rubin et al 2015 [73], higher than that of the OXY-CC-CL unit proposed.

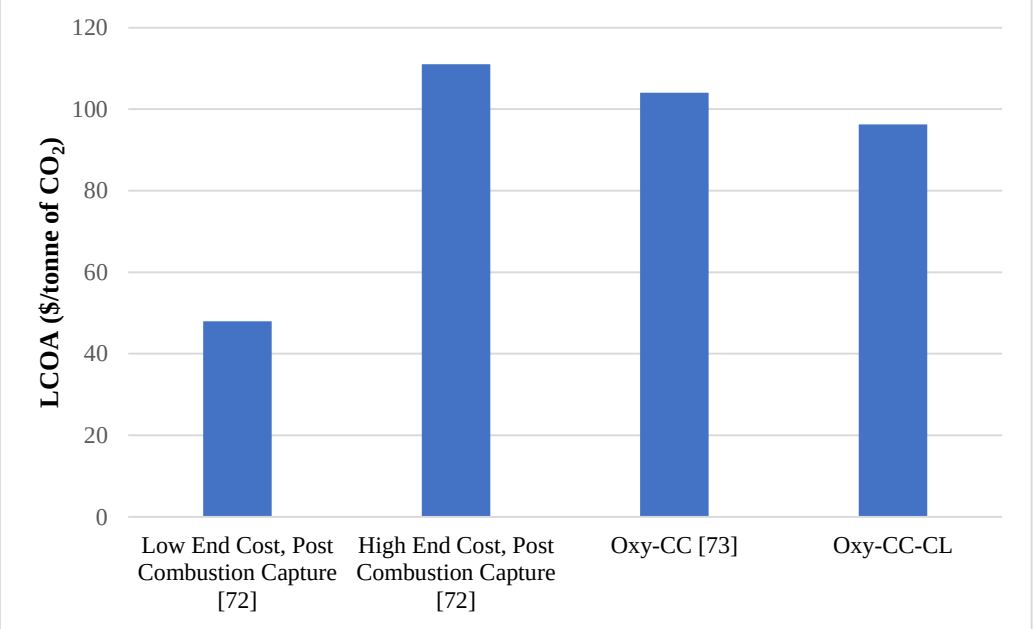

Figure 11. Comparative Evaluation of the Levelized Cost of Carbon Capture between OXY-CC-CL and post-combustion capture at new NGCC power plants

9 Pinch Analysis

The optimization for the proposed OXY-CC-CL plant concept with CCS was performed through heat and power integration analysis (via pinch technique), often used for maximization of power generation [74,75]. A conservative value of 10^{o}C was assumed for the minimum approach temperature, necessary for the pinch assessment [75]. As assumed in the methodology, a simple steam cycle was modelled with the primary aim to obtain the relative efficiency gain from integrating the CL unit to a conventional oxyfuel power plant with CCS. A self-sustained system with regards to thermal integration was obtained. Furthermore, as illustrated from the Hot and Cold Composite curve in Figure 12, a strong potential for system optimization to improve the efficiency further was identified through production of steam for power generation.

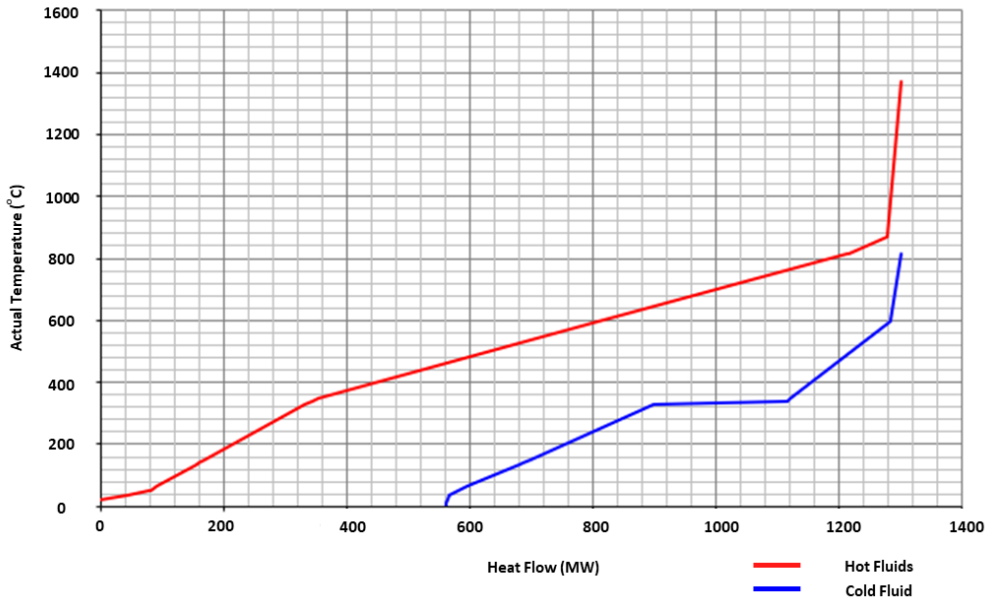

Figure 12. Pinch Analysis of the proposed OXY-CC-CL unit.

About 350 MW thermal of high-temperature heat can be seen to be available for optimized use. Assuming a conservative system efficiency of 30% for electricity generation via steam an additional 105 MW of electricity can be generated by the proposed layout. This would increase the system efficiency to 61.4%, comparable to the state of the art base case NGCC without CCS.

10 Environmental Evaluations

10.1 Water Footprint Analysis

Following the methodology presented in the earlier section, a detailed water demand was calculated for the proposed OXY-CC-CL system. The net specific water footprint was calculated to be 1.893 litres/kWh and more detailed results for water need analysis is summarized in Table 12. As can be seen from Figure 13, the net specific water need of the proposed OXY-CC-CL system is comparable to existing commercial power plant technologies [76]. However, compared to NGCC, the increase of water need is almost 2.5 times. Considering water sustainability, hence the proposed system lags behind and system optimization focusing on lowering the specific water requirement hence are necessary.

Table 12. Summary of Water footprint analysis of the OXY-CC-CL unit.

Description	Unit	Values
LHV of NG	MJ/kg	48.3
Flow of NG	tonne/hr	73.75
Plant Capacity	MW	500.69
Heat Rate (HR)	kJ/kWh	7114.432
Electricity produced	kJ/kWh	3600
Other Heat Losses	kJ/kWh	355.722
Net Energy Out (B)	kJ/kWh	3955.722
Water needed for cooling using tower cooling (A)	litre/kJ	0.001
Specific Cooling Water Requirement	litre/kWh	1.589
Plant Capacity Factor		85%
Net Energy Generated	MWh	3,728,137.74
Total Cooling Water Requirement	m^3	5,923,382.20
Process Water (gross)	litre/kWh	0.2
Gross Plant Capacity	MW	761.74
Gross Energy Generated	MWh	5,671,916.04
Excess Water need for Chemical Looping	litre	0
Total Process Water Requirement	m^3	1,134,383.21
Total Water Footprint	m^3	7,057,765.41
Net Specific Water Footprint	litre/kWh	1.893

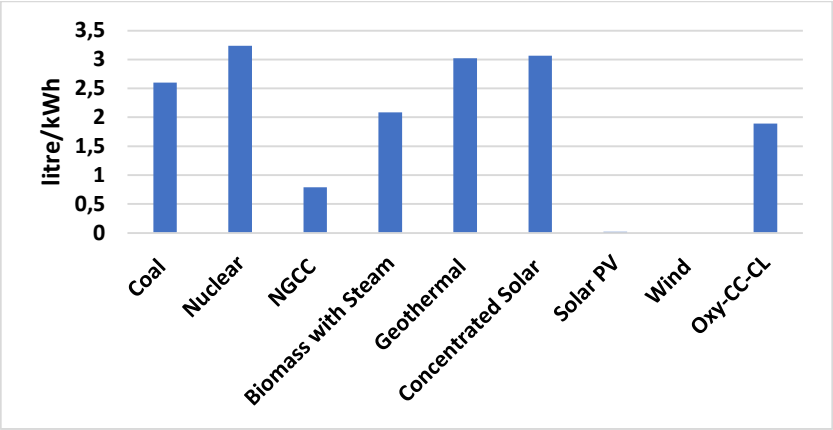

Figure 13. Comparison of specific water need of power production of the proposed OXY-CC-CL and commercial technologies with cooling tower based cooling

10.2 **Land Footprint Analysis**

Comparative Land Footprint Analysis, as presented in Table 13, clearly indicates the larger area needed for similar power production from the three units. The proposed OXY-CC-CL unit, comprising of ASU, CL units and additional metal handling units, with a higher number of turbines, would require a much higher land area. Indeed, it would need as much as 2.5 times the land area than a simple NGCC power plant without carbon capture. The CO_2 drying and compression unit accounts for largest share of the increased area, followed by the chemical looping unit, accounting for about 15% of the total land area needed for the proposed power plant. The ASU, on the other hand, takes up around 7% of the total land area, is considered as a separate unit to the NGCC, connected through pipelines supplying oxygen for combustion.

Table 13. Comparative Land Area Requirement in m^2 for NGCC, OXY-CC and OXY-CC-CL unit for a net power output of 500MW

Component	NGCC	OXY-CC	OXY-CC-CL
NGCC (Combustion Turbine)	1689.078	1689.078	1689.078
ASU		323.13	286.087
CO_2 Drying and Compression		1288.038	1288.038

Chemical Looping Unit - Included as Boiler Units			582.254
Solids Handling Units - Included as equivalent to Coal Handling Plants			210.854
Net Spatial Footprint	1689.078	3300.246	4056.311

Conclusions

Thermochemical looping of ceria for splitting CO_2/H_2O in a methane driven redox cycle producing syngas is integrated with oxyfuel-combustion natural gas combined cycle (OXY-CC-CL). Except the chemical looping CO_2/H_2O dissociation unit (consisting of two interconnected reactors), which is still under technological development, the remaining process design comprises already existing industrial components. The resulting improvement in the system efficiency, even with carbon capture and storage is observed. A system design and simulation were performed in ASPEN Plus to evaluate the thermodynamic performance of the proposed system. An energetic efficiency of 50.7% and an exergetic efficiency of 47.4% was obtained. Sensitivity analysis with different operating parameters of the system showed scopes for improvement, however, subject to development of corresponding technologies. Comparison with natural gas oxyfuel power plant with carbon capture (OXY-CC) revealed a net efficiency gain of around 7.5 percentage points even with 100% CCS, making this technology promising for subsequent applications in future. An economic analysis was further performed and compared with the existing technologies for power production. Even though the specific overnight capital cost was high, at 2455$/kW, the levelized cost of CO_2 savings was obtained as 96.25 $/tonne$CO_2$, well within limits of commercial technologies. An LCOE of 128.01 $/MWh was calculated without carbon tax, which however, would drop to the rates of existing wholesale electricity prices with a carbon tax of around 6 $/tonne$CO_2$. However, as per the pinch analysis performed, with better heat integration, the system efficiency can be improved to almost 56%, resulting in much improved performance of the proposed system. In comparison to NGCC without carbon capture, both the water and land footprints for the proposed technology was obtained to be more than 2.5 times higher for the same scale.

References

[1] J.G.J. (PBL) Olivier, G. (EC-J. Janssens-Maenhout, M. (EC-J. Muntean, J.A.H.W. (PBL) Peters, Trends in Global CO_2 Emissions: 2016 Report, PBL Netherlands Environ. Assess. Agency Eur. Comm. Jt. Res. Cent. (2016) 86. http://edgar.jrc.ec.europa.eu/news_docs/jrc-2016-trends-in-global-co2-emissions-2016-report-103425.pdf.

[2] R.P. Cabral, N. Mac Dowell, A novel methodological approach for achieving £/MWh cost reduction of CO2 capture and storage (CCS) processes, Appl. Energy. 205 (2017) 529–539. doi:10.1016/j.apenergy.2017.08.003.

[3] C. Le Quere, Global carbon budget 2017, Earth Syst. Sci. Data Discuss. 0 (2017). http://www.globalcarbonproject.org/carbonbudget/index.htm.

[4] IPCC, Foreword, Preface, Dedication and In Memoriam, Clim. Chang. 2014 Mitig. Clim. Chang. Contrib. Work. Gr. III to Fifth Assess. Rep. Intergov. Panel Clim. Chang. (2014) 1454. doi:10.1017/CBO9781107415416.

[5] EIA, International Energy Outlook 2017 Overview, U.S. Energy Inf. Adm. IEO2017 (2017) 143. doi:www.eia.gov/forecasts/ieo/pdf/0484(2016).pdf.

[6] P. Viebahn, D. Vallentin, S. Höller, Prospects of carbon capture and storage (CCS) in China's power sector - An integrated assessment, Appl. Energy. 157 (2015) 229–244. doi:10.1016/j.apenergy.2015.07.023.

[7] M.E. Boot-Handford, J.C. Abanades, E.J. Anthony, M.J. Blunt, S. Brandani, N. Mac Dowell, J.R. Fernández, M.-C. Ferrari, R. Gross, J.P. Hallett, R.S. Haszeldine, P. Heptonstall, A. Lyngfelt, Z. Makuch, E. Mangano, R.T.J. Porter, M. Pourkashanian, G.T. Rochelle, N. Shah, J.G. Yao, P.S. Fennell, Carbon capture and storage update, Energy Environ. Sci. 7 (2014) 130–189. doi:10.1039/C3EE42350F.

[8] N. MacDowell, N. Florin, A. Buchard, J. Hallett, A. Galindo, G. Jackson, C.S. Adjiman, C.K. Williams, N. Shah, P. Fennell, An overview of CO2 capture technologies, Energy Environ. Sci. 3 (2010) 1645. doi:10.1039/c004106h.

[9] C.M. Quintella, S.A. Hatimondi, A.P.S. Musse, S.F. Miyazaki, G.S. Cerqueira, A. De Araujo Moreira, CO2 capture technologies: An overview with technology assessment based on patents and articles, Energy Procedia. 4 (2011) 2050–2057. doi:10.1016/j.egypro.2011.02.087.

[10] J. Gibbins, H. Chalmers, Carbon capture and storage, Energy Policy. 36 (2008) 4317–4322. doi:10.1016/j.enpol.2008.09.058.

[11] D.J. Dillon, V. White, R.J. Allam, R.A. Wall, J. Gibbins, Oxy Combustion Processes for CO2 Capture from Power Plant, (2005).

[12] A. Bose, K. Jana, D. Mitra, S. De, Co-production of power and urea from coal with CO2 capture: Performance assessment, Clean Technol. Environ. Policy. 17 (2015). doi:10.1007/s10098-015-0960-7.

[13] Q. Zhang, Nurhayati, C.L. Cheng, D. Nagarajan, J.S. Chang, J. Hu, D.J. Lee, Carbon capture and utilization of fermentation CO2: Integrated ethanol fermentation and succinic acid production as an efficient platform, Appl. Energy. 206 (2017) 364–371. doi:10.1016/j.apenergy.2017.08.193.

[14] C. Graves, S.D. Ebbesen, M. Mogensen, K.S. Lackner, Sustainable hydrocarbon fuels by recycling CO2and H2O with renewable or nuclear energy, Renew. Sustain. Energy Rev. 15 (2011) 1–23. doi:10.1016/j.rser.2010.07.014.

[15] R.W. Breault, E.R. Monazam, J.T. Carpenter, Analysis of hematite re-oxidation in the chemical looping process, Appl. Energy. 157 (2015) 174–182. doi:10.1016/j.apenergy.2015.08.015.

[16] C. Zhou, K. Shah, H. Song, J. Zanganeh, E. Doroodchi, B. Moghtaderi, Integration Options and Economic Analysis of an Integrated Chemical Looping Air Separation Process for Oxy-fuel Combustion, Energy & Fuels. 30 (2016) 1741–1755. doi:10.1021/acs.energyfuels.5b02209.

[17] C. Yin, J. Yan, Oxy-fuel combustion of pulverized fuels: Combustion fundamentals and modeling, Appl. Energy. 162 (2016) 742–762. doi:10.1016/j.apenergy.2015.10.149.

[18] S. Mukherjee, P. Kumar, A. Yang, P. Fennell, Energy and exergy analysis of chemical looping combustion technology and comparison with pre-combustion and oxy-fuel combustion technologies for CO<inf>2</inf> capture, J. Environ. Chem. Eng. 3 (2015) 2104–2114. doi:10.1016/j.jece.2015.07.018.

[19] K. Shah, B. Moghtaderi, J. Zanganeh, T. Wall, Integration options for novel chemical looping air separation (ICLAS) process for oxygen production in oxy-fuel coal fired power plants, Fuel. 107 (2013) 356–370. doi:10.1016/j.fuel.2013.01.007.

[20] I. Pfaff, A. Kather, Comparative thermodynamic analysis and integration issues of CCS

steam power plants based on oxy-combustion with cryogenic or membrane based air separation, Energy Procedia. 1 (2009) 495–502. doi:10.1016/j.egypro.2009.01.066.

[21] J.-P. Tranier, R. Dubettier, N. Perrin, Air Liquide, Air Separation Unit for Oxy-Coal Combustion Systems, 1st Int. Oxyfuel Combust. Conf. (2009).

[22] B. Moghtaderi, A Novel Chemical Looping Based Air Separation Technology for Oxy-Fuel Combustion of Coal, 2014. doi:10.1115/1.802915.ch1.

[23] A.E. Farooqui, H.M. Badr, M.A. Habib, R. Ben-Mansour, Numerical investigation of combustion characteristics in an oxygen transport reactor, Int. J. Energy Res. 38 (2014). doi:10.1002/er.3070.

[24] A.E. Farooqui, M.A. Habib, H.M. Badr, R. Ben-Mansour, Modeling of ion transport reactor for oxy-fuel combustion, Int. J. Energy Res. 37 (2013). doi:10.1002/er.2923.

[25] R. Ben-Mansour, M.A. Habib, H.M. Badr, F. Azharuddin, M. Nemitallah, Characteristics of oxy-fuel combustion in an oxygen transport reactor, in: Energy and Fuels, ACS Publications, 2012: pp. 4599–4606. doi:10.1021/ef300539c.

[26] A. Skorek-Osikowska, Ł. Bartela, J. Kotowicz, Thermodynamic and ecological assessment of selected coal-fired power plants integrated with carbon dioxide capture, Appl. Energy. 200 (2017) 73–88. doi:10.1016/j.apenergy.2017.05.055.

[27] C.C. Cormos, Evaluation of syngas-based chemical looping applications for hydrogen and power co-generation with CCS, Int. J. Hydrogen Energy. 37 (2012) 13371–13386. doi:10.1016/j.ijhydene.2012.06.090.

[28] R. Stanger, T. Wall, R. Spörl, M. Paneru, S. Grathwohl, M. Weidmann, G. Scheffknecht, D. McDonald, K. Myöhänen, J. Ritvanen, Oxyfuel combustion for CO 2 capture in power plants, Int. J. Greenh. Gas Control. 40 (2015) 55–125.

[29] J. Mletzko, S. Ehlers, A. Kather, Comparison of natural gas combined cycle power plants with post combustion and oxyfuel technology at different CO2 capture rates, Energy Procedia. 86 (2016) 2–11. doi:10.1016/j.egypro.2016.01.001.

[30] S. Nazir, O. Bolland, S. Amini, Analysis of Combined Cycle Power Plants with Chemical Looping Reforming of Natural Gas and Pre-Combustion CO2 Capture, Energies. 11 (2018) 147. doi:10.3390/en11010147.

[31] A. Le Gal, S. Abanades, G. Flamant, CO 2 and H 2 O Splitting for Thermochemical Production of Solar Fuels Using Nonstoichiometric Ceria and Ceria/Zirconia Solid

Solutions, Energy & Fuels. 25 (2011) 4836–4845. doi:10.1021/ef200972r.

[32] A.E. Farooqui, A.M. Pica, P. Marocco, D. Ferrero, A. Lanzini, S. Fiorilli, J. Llorca, M. Santarelli, Assessment of kinetic model for ceria oxidation for chemical-looping CO2dissociation, Chem. Eng. J. 346 (2018) 171–181. doi:10.1016/j.cej.2018.04.041.

[33] P.T. Krenzke, J.H. Davidson, Thermodynamic analysis of syngas production via the solar thermochemical cerium oxide redox cycle with methane-driven reduction, Energy and Fuels. 28 (2014) 4088–4095. doi:10.1021/ef500610n.

[34] M. Welte, K. Warren, J.R. Scheffe, A. Steinfeld, Combined Ceria Reduction and Methane Reforming in a Solar-Driven Particle-Transport Reactor, Ind. Eng. Chem. Res. 56 (2017) 10300–10308. doi:10.1021/acs.iecr.7b02738.

[35] S. Mukherjee, P. Kumar, A. Yang, P. Fennell, A systematic investigation of the performance of copper-, cobalt-, iron-, manganese- and nickel-based oxygen carriers for chemical looping combustion technology through simulation models, Chem. Eng. Sci. 130 (2015) 79–91. doi:10.1016/j.ces.2015.03.009.

[36] S. Nasr, The reduction kinetics of iron oxide ore by methane for chemical-looping combustion, (2012).

[37] R.J. Carrillo, J.R. Scheffe, Advances and trends in redox materials for solar thermochemical fuel production, Sol. Energy. 156 (2017) 3–20. doi:10.1016/j.solener.2017.05.032.

[38] A. Steinfeld, Solar thermochemical production of hydrogen - A review, Sol. Energy. 78 (2005) 603–615. doi:10.1016/j.solener.2003.12.012.

[39] J.R. Scheffe, A. Steinfeld, Oxygen exchange materials for solar thermochemical splitting of H2O and CO2: A review, Mater. Today. 17 (2014) 341–348. doi:10.1016/j.mattod.2014.04.025.

[40] D. Yadav, R. Banerjee, A review of solar thermochemical processes, Renew. Sustain. Energy Rev. 54 (2016) 497–532. doi:10.1016/j.rser.2015.10.026.

[41] S. Lorentzou, G. Karagiannakis, D. Dimitrakis, C. Pagkoura, A. Zygogianni, A.G. Konstandopoulos, Thermochemical Redox Cycles over Ce-based Oxides, Energy Procedia. 69 (2015) 1800–1809. doi:10.1016/j.egypro.2015.03.152.

[42] F. Liu, Cerium oxide promoted oxygen carrier development and scale modeling study for chemical looping comustion, (2013).

[43] S.M. Nazir, O. Bolland, S. Amini, Full Plant Scale Analysis of Natural Gas Fired Power Plants with Pre-Combustion CO2 Capture and Chemical Looping Reforming (CLR), Energy Procedia. 114 (2017) 2146–2155. doi:10.1016/j.egypro.2017.03.1350.

[44] K.J. Warren, J.R. Scheffe, Kinetic insights into the reduction of ceria facilitated via the partial oxidation of methane, Mater. Today Energy. 9 (2018) 39–48. doi:10.1016/j.mtener.2018.05.001.

[45] D.P. Harrison, Sorption-Enhanced Hydrogen Production : A Review, (2008) 6486–6501.

[46] HYGHSPIN, Flexible use – maximum efficiency : Gentle product handling plus CIP with one and the same pump !, n.d.

[47] M.N. Khan, T. Shamim, Influence of Specularity Coefficient on the Hydrodynamics and Bubble Statistics of an Annular Fluidized Bed Reactor, Energy Procedia. 105 (2017) 1998–2003. doi:10.1016/j.egypro.2017.03.573.

[48] J. Fan, L. Zhu, P. Jiang, L. Li, H. Liu, Comparative exergy analysis of chemical looping combustion thermally coupled and conventional steam methane reforming for hydrogen production, J. Clean. Prod. 131 (2016) 247–258. doi:10.1016/j.jclepro.2016.05.040.

[49] Politecnico di Milano - CAESER Project, European best practice guidelines for assessment of CO2 capture technologies, 2011.

[50] G.P. Hammond, Engineering sustainability : thermodynamics , energy systems , and the environment, 639 (2004) 613–639. doi:10.1002/er.988.

[51] J. Szargut, Chemical Exergies of the Elements, Appl. Energy. 32 (1989) 269–286.

[52] M.N. Khan, T. Shamim, Exergoeconomic analysis of a chemical looping reforming plant for hydrogen production, Int. J. Hydrogen Energy. 42 (2017) 4951–4965. doi:10.1016/j.ijhydene.2016.11.098.

[53] J.Y. Xiang, M. Cal, M. Santarelli, Calculation for physical and chemical exergy of flows in systems elaborating mixed-phase flows and a case study in an IRSOFC plant, 115 (2004) 101–115. doi:10.1002/er.953.

[54] A. Bejan, Thermal Design and Optimzation, John Wiley, New York, 1996.

[55] T.J. Kotas, The Exergy Method of Thermal Plant Analysis, Butterworths, 1985.

[56] S. Sievers, T. Seifert, M. Franzen, G. Schembecker, C. Bramsiepe, Fixed capital investment estimation for modular production plants, Chem. Eng. Sci. 158 (2017) 395–410. doi:10.1016/j.ces.2016.09.029.

[57] C. Cormos, Integrated assessment of IGCC power generation technology with carbon capture and storage (CCS), Energy. 42 (2012) 434–445. doi:10.1016/j.energy.2012.03.025.

[58] R. Porrazzo, G. White, R. Ocone, Techno-economic investigation of a chemical looping combustion based power plant, Faraday Discuss. 192 (2016) 437–457. doi:10.1039/C6FD00033A.

[59] Y. Zhao, H. Chen, M. Waters, D.N. Mavris, Modeling and Cost Optimization of Combined Cycle Heat Recovery Generator Systems, Vol. 1 Turbo Expo 2003. (2003) 881–891. doi:10.1115/GT2003-38568.

[60] N. Berghout, T. Kuramochi, M. van den Broek, A. Faaij, Techno-economic performance and spatial footprint of infrastructure configurations for large scale CO2 capture in industrial zones. A case study for the Rotterdam Botlek area (part A), Int. J. Greenh. Gas Control. 39 (2015) 256–284. doi:10.1016/j.ijggc.2015.05.019.

[61] IEA, Executive Summary - Projected Costs of Generating Electricity, 2015.

[62] Eurostat, Natural gas price statistics, EU-28, (2016) 1–12. doi:http://ec.europa.eu/eurostat/statistics-explained/index.php/Natural_gas_price_statistics.

[63] M.M. Mekonnen, P.W. Gerbens-Leenes, A.Y. Hoekstra, The consumptive water footprint of electricity and heat: a global assessment, Environ. Sci. Water Res. Technol. 1 (2015) 285–297. doi:10.1039/C5EW00026B.

[64] A.D. Martin, A. Delgado, A. Delgado Martin, Water Footprint of Electric Power Generation : Modeling its use and analyzing options for a water-scarce future, 2012. doi:10.1021/es802162x.

[65] N. Florin, P. Fennell, CCR Land Footprint Review, IC 26, (2006) 1–30. https://www.gov.uk/government/uploads/system/uploads/attachment_data/file/43615/CCR_guidance_-_Imperial_College_review.pdf.

[66] M. Ishida, H. Jin, A novel chemical-looping combustor without NOx formation, Ind. Eng. Chem. Res. 35 (1996) 2469–2472. doi:10.1021/ie950680s.

[67] Wärtsilä, Gas Turbine for Power Generation: Introduction, (2018). https://www.wartsila.com/energy/learning-center/technical-comparisons/gas-turbine-for-power-generation-introduction (accessed May 29, 2018).

[68] M. Pan, F. Aziz, B. Li, S. Perry, N. Zhang, I. Bulatov, R. Smith, Application of optimal design methodologies in retrofitting natural gas combined cycle power plants with CO2capture, Appl. Energy. 161 (2016) 695–706. doi:10.1016/j.apenergy.2015.03.035.

[69] U.S.D. of Energy, Capital Cost Estimates for Utility Scale Electricity Generating Plants, (2016). https://www.eia.gov/analysis/studies/powerplants/capitalcost/pdf/capcost_assumption.pdf.

[70] U.S.D. of Energy, Capital Cost Estimates for Utility Scale Electricity Generating Plants, (2016).

[71] Market Observatory for Energy, Quarterly Report on on European Electricity Markets, 2017.

[72] Z. Khorshidi, M. Soltanieh, Y. Saboohi, M. Arab, Economic Feasibility of CO 2 Capture from Oxy-fuel Power Plants Considering Enhanced Oil Recovery Revenues, Energy Procedia. 4 (2011) 1886–1892. doi:10.1016/j.egypro.2011.02.067.

[73] E.S. Rubin, J.E. Davison, H.J. Herzog, The cost of CO 2 capture and storage, Int. J. Greenh. Gas Control. (2015). doi:10.1016/j.ijggc.2015.05.018.

[74] J. Varghese, S. Bandyopadhyay, Targeting for energy integration of multiple fired heaters, Ind. Eng. Chem. Res. 46 (2007) 5631–5644. doi:10.1021/ie061619y.

[75] C.C. Cormos, Evaluation of energy integration aspects for IGCC-based hydrogen and electricity co-production with carbon capture and storage, Int. J. Hydrogen Energy. 35 (2010) 7485–7497. doi:10.1016/j.ijhydene.2010.04.160.

[76] E.S. Spang, W.R. Moomaw, K.S. Gallagher, P.H. Kirshen, D.H. Marks, The water consumption of energy production : an international comparison, (2014). doi:10.1088/1748-9326/9/10/105002.